이학박사 학위논문

A study on roles of microRNA-188 in dendritic plasticity and its pathophysiological significance in Alzheimer's disease

마이크로알엔에이-188 의 수상돌기 가소성에서의 역할 및 알츠하이머병에서의 병태생리적 의미에 관한 연구

2014 년 02 월

서울대학교 대학원

의과학과

이 기 환

A thesis of the Degree of Doctor of Philosophy in Science

마이크로알엔에이-188 의 수상돌기 가소성에서의 역할 및 알츠하이머병에서의 병태생리적 의미에 관한 연구

A study on roles of microRNA-188 in dendritic plasticity and its pathophysiological significance in Alzheimer's disease

Feb. 2014

The Department of Biomedical Sciences,
Seoul National University Graduate School
Kihwan Lee

마이크로알엔에이-188 의 수상돌기 가소성에서의 역할 및 알츠하이머병에서의 병태생리적 의미에 관한 연구

지도 교수 김 혜 선

이 논문을 이학박사 학위논문으로 제출함
2013년 10월

서울대학교 대학원
의과학과 분자신경약리전공
이 기 환

이기환의 이학박사 학위논문을 인준함
2013년 12월

위 원 장 _____ (인)

부위원장 _____ (인)

위 원 _____ (인)

위 원 _____ (인)

위 원 _____ (인)

A study on roles of microRNA-188 in dendritic plasticity and its pathophysiological significance in Alzheimer's disease

by
Kihwan Lee

A thesis submitted to the Department of Biomedical Sciences in partial fulfillment of the requirements for the Degree of Doctor of Philosophy in Sciences at Seoul National University Graduate School

Dec. 2013

Approved by Thesis Committee:

Professor _____ **Chairman**

Professor _____ **Vice chairman**

Professor _____

Professor _____

Professor _____

ABSTRACT

Introduction: In the central nervous system (CNS), miRNAs have been shown to regulate development, survival, function and plasticity. Despite considerable evidence for the regulatory functions of miRNAs, the identities of the miRNA species that are involved in the regulation of synaptic transmission and plasticity and the mechanisms by which these miRNAs exert their functional roles remain largely unknown. Moreover, neurodegenerative diseases, such as Alzheimer's disease (AD), may be primarily a disorder derived from synaptic failure through dysfunction of dendritic spine and synaptic transmission, finally resulting in cognitive dysfunction. The goal of this study is to investigate the changes of miRNAs during long-term potentiation (LTP) induction and regulatory mechanisms or miRNAs in terms of dendritic plasticity in rat hippocampus. In addition, I also tried to examine pathophysiological roles of miR-188, one of miRNAs of which expression has been altered during LTP induction, in AD.

Methods: To investigate the changes in expression profiles of miRNAs during LTP in rat hippocampal acute slice, miRNAs microarray and RT-qPCR were performed. Based on the profiled miRNAs microarray data, potential targets for miRNAs, of which expression were altered by LTP, were sought using bioinformatic programs. I examined the effects of miR-188, whose expression was upregulated by LTP and targets neuropilin-2 (Nrp-2), on dendritic spine density in rat primary hippocampal neuron cultures. Next, to investigate the pathophysiological roles of miR-188 in cognitive

dysfunction in AD, first the levels of expression of miR-188 in the brains from human AD patients and 5x familial AD (5 x FAD) animal model were determined. I also examined whether oligomeric beta amyloid 1-42 ($oA\beta_{1-42}$) affected the expression of miR-188 and whether miR-188 rescues the reduction in dendritic spine density induced by $oA\beta_{1-42}$ in rat primary hippocampal neuron cultures. In addition, T-maze and contextual fear conditioning tests were performed with 5 x FAD AD animal model 3 weeks after viral-mediated expression of miR-188 in hippocampal CA1 region.

Results: The expression of miR-188 was found to be upregulated by LTP induction. The protein level of Nrp-2, one of possible molecular targets for miR-188, was decreased during LTP induction. I also confirmed that the luciferase activity of the 3'-untranslated region (UTR) of Nrp-2 was diminished by treatment with a miR-188 oligonucleotide but not with a scrambled miRNA oligonucleotide. Nrp-2 serves as a receptor for semaphorin 3F (Sema3F), which is a negative regulator of spine development and synaptic structure. In addition, miR-188 specifically rescued the reduction in dendritic spine density induced by Nrp-2 expression in rat primary hippocampal neuron cultures.

miR-188 was significantly downregulated in the cerebral cortices (medial frontal gyrus) and hippocampi from AD patients, compared to those from age-matched control subjects. In addition, immunoreactivity against Nrp-2 was highly upregulated in the brain from AD patients, compared to those from age-matched control subjects. I also demonstrated that the treatment with $oA\beta_{1-42}$ significantly diminisheed the expression of miR-188 whereas the

treatment of brain-derived neurotrophic factor significantly upregulated the expression of miR-188 in primary hippocampal neuron cultures. The treatment with miR-188 rescued the reduction in dendritic spine induced by oAβ_{1-42} in rat primary hippocampal neuron cultures. In addition, I found that viral-mediated expression of miR-188 into hippocampal CA1 ameliorated the cognitive impairment in 5 x FAD mice.

Conclusions: I showed that an activity-dependent miRNA, miR-188, regulates dendritic plasticity by downregulating Nrp-2, which was known to be a negative regulator of dendritic spine formation and synaptic transmission. In addition, I demonstrated that the reduction in the expression of miR-188 in the brains from AD patients and AD animal model may contribute to the cognitive dysfunction observed in the disease.

Taken together, this study provides that miR-188 act as an important regulator contributing to dendritic plasticity by downregulating Nrp-2 in synaptic functions. In addition, deficiency in miR-188 expression results in the reduction in dendritic spine numbers and accelerates cognitive impairment in AD. Therefore, I suggest that miR-188 has a therapeutic potential for AD, and could be developed as a diagnostic biomarker for the disease.

Keywords: MicroRNAs, Synaptic plasticity, Neuropilin-2, Cognitive impairment, Alzheimer's disease

Student number: 2008-31030

CONTENTS

LIST OF FIGURES

Chapter 1 (Role of miR-188 in dendritic plasticity)

Chapter 2 (Pathophysiological role of miR-188 in AD)

LIST OF ABBREVIATIONS

aCSF: artificial CSF AD: Alzheimer's disease

ADAM: a disintergrin and metalloproteinase

AMPAR: α-amino-3-hydroxy-5-methyl-4-isoxazolepropionic acid receptor

AP: action potential APH-1: anterior pharynx-defective 1

APP: amyloid precursor protein BACE-1: β-site APP cleaving enzyme-1

BDNF: brain-derived neurotrophic factor

CFC: contextual fear conditioning

chem-LTP: chemical long-term potentiation

CNS: central nervous system CSF: cerebrospinal fluid

DG: dentate gyrus

DGCR8: DiGeorge Syndrome Critical Region 8

DIV: day *in vitro*

DMEM: Dulbecco's modified Eagle's medium

DMSO: dimethyl sulfoxide ECL: enhanced chemiluminescent

EPSCs: excitatory postsynaptic currents

EPSPs: excitatory postsynaptic potentials

fEPSP: field recording of EPSP FV: fiber volley amplitude

GCs: granule cells GAP 43: growth associated protein 43

HEK 293: human embryonic kidney 293

HFIP: 1,1,1,3,3,3-hexafluoro-2-propanol

HPC: hippocampus HRP: horse-radish peroxidase

I/O curve: Input/output curve

IRES: internal ribosome entry site KO: knockout

LimK1: Lim domain kinase 1 LTP: long-term potentiation

LTD: long-term depression

mGluR-LTD: metabotropic glutamate receptor (mGluR)

miRNA: microRNA

miR-SC: scrambled miRNA oligonucleotide

MFG: medial frontal gyrus NFT: neurofibrillary tangle

NMDAR: N-methyl-d-aspartic acid receptor

Nrps: neuropilins Nrp-2: neuropilins-2

NTs: neurotransmitters

oA$\beta_{1\text{-}42}$: oligomeric beta amyloid 1-42 peptide

PEN-2: presenilin enhancer 2 PLGF: placenta growth factor

PTX: picrotoxin RISC: RNA-induced silencing complex

RNA pol II: RNA polymerase II

RT-PCR: reverse transcription polymerase chain reaction

RT-qPCR: quantitative real time RT-PCR

SC: schaffer collateral SEM: standard error of means

Sema3: class 3 of semaphoring TG: transgenic

TRBP: transactivating response (TAR) RNA-binding protein

UTR: untranslated region VEGF: vascular endothelial growth factor

WT: wild-type

2’-O-Me RNA: oligonucleotide with methyl group at their 2’-OH residue

2’-O-Me-188-AS: antisense 2’-O-Me oligonucleotide for miR-188

5 x FAD: 5 x familial Alzheimer’s disease

GENERAL INTRODUCTION

miRNAs

miRNAs are 21-25 nucleotide-long small non-coding RNAs that negatively regulate gene expression at the post-transcriptional level (1-3). miRNAs are conserved throughout higher eukaryotes (i.e., animals and plants) (2, 4-6). Members of the miRNA family were initially discovered as small temporal RNAs that regulate developmental transitions, such as the timing of larval development in *Caenorhabditis elegans* (7-9).

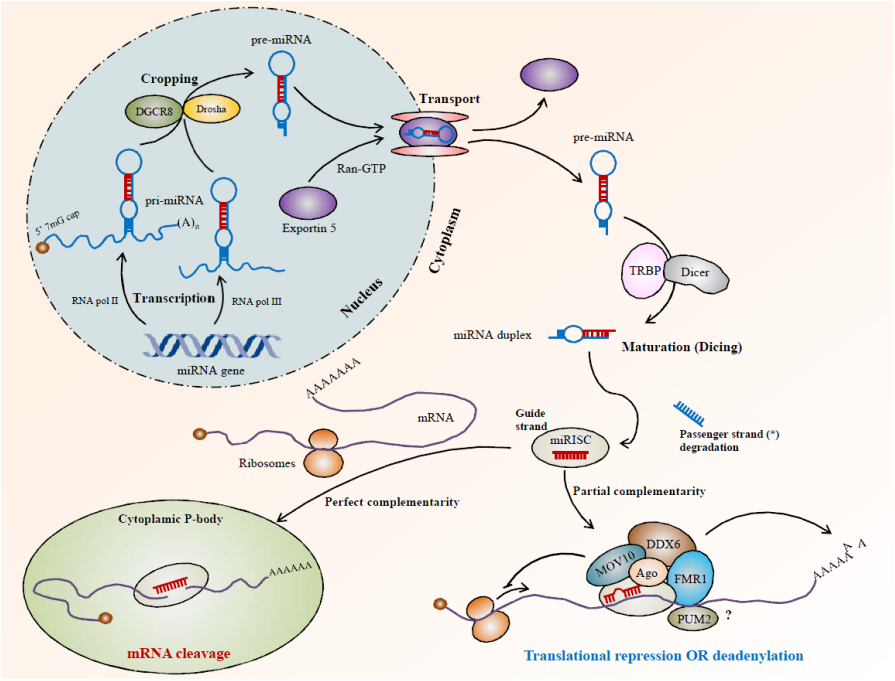

Fig. 1-1. A schematic diagram of microRNA biogenesis

The transcription of miRNA genes mediated by RNA polymerase II (RNA pol II; See Fig. 1-1) (10, 11) yields primary miRNAs that are usually hundreds to

several thousand nucleotides long and contain a local hairpin structure. The primary miRNA transcripts contain cap structures and poly (A) tails, which are unique properties of the gene transcripts produced by RNA pol II. However, other pathways generate a minor set of miRNAs that are primarily derived from genomic repeats. For example, RNA pol III is responsible for the transcription of miRNA from Alu repeats (12).

The production of miRNAs involves the stepwise processing of the primary transcripts of miRNA genes. Briefly, the stem-loop structures of the primary transcripts are cropped by the nuclear RNase III Drosha-DiGeorge syndrome critical region 8 (DGCR8 or “Pasha” in invertebrates) complex (Microprocessor) (13-16), which is a member of the RNase III class, in the nucleus into stem-looped RNAs of ~65 nucleotides in length, which are termed precursor miRNAs (17, 18). The precursor-miRNAs contain the mature miRNAs that are ~22 nucleotides in length in either the 5' or 3' half of their stem, and the pair of crops performed the by Drosha-DGCR8 complex establishes either the 5' or the 3' end of the mature miRNA. Precursor-miRNAs are exported from the nucleus to the cytoplasm by Exportin-5, which is a member of the RanGTP-dependent nuclear transport receptor family (19-22).

In the cytoplasm, precursor-miRNAs are further processed by Dicer, another member of the RNase III enzyme family (23-27), to produce miRNA duplexes of ~21 nucleotides in length. Typically, of the two RNA strands in the duplex, only one is selectively incorporated into a miRNA-containing ribonucleoprotein complex, known as the RNA-induced silencing complex

(RISC), where it acts to guide RISC to mRNAs that bear complementary sequences (28-30). RISC is composed of Dicer; the human immunodeficiency virus-1 transactivating response (TAR) RNA-binding protein (TRBP) (31), which is a double-stranded RNA binding protein; and Argonaute2 (Ago2) (32, 33). RISC identifies target mRNAs based on the complementarity between a single-stranded miRNA (i.e., the guide-strand miRNA) and the target mRNA. The seed sequence located 2-8 nucleotides from the 5' end of the miRNA plays a pivotal role in binding to the target mRNA (2, 34).

Recent reports have suggested that miRNAs play key roles in diverse biological phenomena, including cellular differentiation, proliferation, development, survival and apoptosis (35, 36). Some miRNAs are specifically expressed and enriched in the brain and have thus been implicated in memory, neuronal differentiation, and synaptic plasticity (37-44).

For example, miR-124 is enriched in the brain and promotes neuronal gene expression in differentiating neural progenitor cells (45). Moreover, miR-124 expression is inhibited by the repressor element 1-silencing transcription factor (46), and miR-124 promotes the neuronal differentiation of progenitor cells into mature neurons by regulating a repressor of alternative pre-mRNA splicing in non-neuronal cells (47). miR-133b is enriched in dopaminergic neurons of the mammalian midbrain where it regulates the maturation and function of midbrain dopaminergic neurons through a negative feedback circuit that involves the transcription factor Pituitary homeobox 3 (44).

Moreover, miR-134 is localized to the synaptodendritic compartments of hippocampal neurons and regulates synaptic plasticity by inhibiting the

translation of Lim domain kinase 1 (LimK1) (48). Importantly, brain-derived neurotrophic factor (BDNF) may trigger neuroplasticity by reversing the translational block of LimK1 by miR-134, which limits the dendritic spine size (48). Moreover, other miRNAs that have been shown to regulate dendritic spine formation include miR-138, which represses the expression of acyl protein thioesterase 1 to negatively regulate spine formation (49); miR-125b, which promotes spine formation (50); and miR-124, which inhibits the expression of cAMP response element-binding protein (40).

Furthermore, other miRNAs that are induced by long-term chemical potentiation (chem-LTP) or long-term metabotropic glutamate receptor depression (mGluR-LTD) provide mechanisms that prevent excess protein synthesis during the expression of synaptic plasticity, which suggests that the extensive regulation of the expressions of miRNAs by chem-LTP and mGluR-LTD plays a critical role in synaptic plasticity (39). However, some of the functions of miRNA in synaptic plasticity have yet to be elucidated. Due to the involvement of miRNAs in synaptic functions and the absence of a known mechanistic link between miRNAs and synaptic plasticity (i.e., LTP and LTD), several researchers have attempted to demonstrate that specific miRNAs function in LTP and to determine the mechanisms by which these miRNAs regulate synaptic strength. Recently, the miRNA expression profiles induced by chem-LTP and chem-LTD were characterized (39); however, the specific mechanisms by which these miRNAs exert their influences on synapses and neurons have not been confirmed.

Therefore, based on extensive study and comparison of the previously

published papers, I designed a method to screen for miRNAs that exhibit altered expression profiles during chem-LTP (39). Next, I employed a bioinformatics approach that utilized a miRNA-target gene prediction algorithm to search for the target genes of these miRNAs and examined the possible interactions between miRNAs and target genes.

It has been reported that the miR-20a family regulates the expression of amyloid precursor protein (APP) *in vitro* and that members of this family function as novel endogenous regulators (51). Moreover, another research group reported that miR-9 and miR-128 are upregulated in the CA1 of the hippocampi of AD patients (52) and that miR-9, miR-29a/29b and miR-107 are downregulated in sporadic AD patients (51, 53).

Synaptic Plasticity

The CNS is composed of two types of specialized cells: neurons and glia. Neurons may have several dendritic branches, but they have at most one axon. Neuronal dendrites have numerous small membrane protrusions called dendritic spines that receive input from presynaptic terminals. Dendritic spines serve as a storage site of changes in synaptic strength. Dendritic spines are highly plastic in terms of shape, volume, and number, and these changes can occur over short time courses.

In the CNS, a synapse is a structure that permits a neuron to pass an electrical or chemical signal to other cells (neural or non-neural). The word "synapse" (from the Greek synapsis meaning "conjunction", which itself is from synaptein meaning "to clasp", in turn comes from syn-, meaning "together", and haptein, meaning "to fasten") was introduced in 1897 by the English physiologist Michael Foster at the suggestion of the English classical scholar Arthur Woollgar Verrall (54). There are two fundamentally different types of synapses. The first is the chemical synapse, and the second is the electrical synapse. In chemical synapses, the arrival of an action potential (AP) at the presynaptic terminal depolarizes the local membrane potential, which activates voltage-gated Ca^{2+} channels that, in turn, lead to an influx of Ca^{2+}. The influx of Ca^{2+} into the presynaptic terminal triggers the fusion of synaptic vesicles that are docked at the plasma membrane facing the synaptic cleft, which is the space that separates the presynaptic and postsynaptic terminals. As each vesicle fuses with the plasma membrane, it releases its content of neurotransmitters (NTs) into the synaptic cleft. The NTs diffuse across the

synaptic cleft and bind to their corresponding receptors in the postsynaptic membrane. L-glutamate is the most commonly utilized NT in the excitatory synapses of the CNS. When released from the synaptic vesicles in the presynaptic terminal of an excitatory synapse, L-glutamate can bind to and activate both metabotropic and ionotropic glutamate receptors, such as AMPA, NMDA, and kainate receptors (collectively referred to as glutamate receptors), that are present along the postsynaptic terminal. The activation of these glutamate receptors triggers a number of phenomena, such as influxes of Na^+ and Ca^{2+} and the release of Ca^{2+} from intracellular storage via intracellular signaling, that converge to increase the cation concentration in the postsynaptic terminal, which in turn result in a localized depolarization of the membrane potential that is termed an excitatory postsynaptic potential (EPSP). The EPSPs that are generated in the postsynaptic terminals and propagated via the dendrites as excitatory postsynaptic currents (EPSCs) are spatially and temporally summed in the soma of the postsynaptic neuron. When the membrane depolarization caused by the accumulated EPSC crosses a threshold in the axon hillock, a specialized structure located between the soma and the axon of the postsynaptic neuron. An AP that can propagate along the axon of the postsynaptic neuron is generated.

Information is stored and retrieved in our brain via a neural code (55). Given that all neural codes in the CNS rely on the propagation of APs from one neuron to another, alterations of the likelihood with which an AP propagated by a presynaptic neuron will result in an AP in a postsynaptic neuron are the basic mechanisms by which the information stored in our brains is modulated;

i.e., these alterations are responsible for the *de novo* generation of new memories and the loss of existing memories. These phenomena are generally termed neuroplasticity (56, 57). One specific mechanism of neuroplasticity is mediated by an increase in the strength of the EPSPs generated in the postsynaptic terminal in response to a given AP that is propagated by the presynaptic neuron. More specifically, such increases in strength can be achieved by altering, either in concert or separately, the properties of the glutamate receptors (e.g., the gating probability) via post-translational modifications and allosteric modulations or the numbers of the glutamate receptors present in the postsynaptic terminal. The alterations that arise from such mechanisms involve changes at the synapse and are specifically referred to as synaptic plasticity to distinguish these alterations from non-synaptic components of neuroplasticity (58, 59). When such synaptic strengthening or "potentiation" is maintained for long periods, it is referred to as long-term potentiation (LTP). Similar mechanisms operating in reverse can also weaken the strength of EPSPs generated at the postsynaptic terminal, and this phenomenon is termed long-term depression (LTD) (60-62). LTP and LTD are examples of synaptic plasticity, which is essentially the ability of synapses to strengthen or weaken the strength of their responses to various stimuli (63, 64). LTP between presynaptic and postsynaptic neurons can be replicated in laboratory settings (60-62). LTP has been extensively characterized using electrophysiological, biochemical and molecular research techniques. LTP has been the most preferentially studied form of synaptic plasticity. Although several recent studies have detected LTP-like synaptic changes in the

amygdala (65) following learning, the hippocampus has been and remains the major experimental system for the study of synaptic plasticity in the context of learning and memory in the brain (66, 67). The importance of studying LTP cannot be underestimated. Not only is LTP important for the study of neuroplasticity, but aberrant changes in LTP are also intimately related to dysfunctions of the entire brain, and alterations or impairments in LTP contribute to many neurological diseases, including depression, Parkinson's disease, epilepsy, neuropathic pain, drug addiction, and AD.

Neuropilin-2

The neuropilins (Nrps) are structurally related molecules that are expressed on the cell surface. Nrps are 130- to 140-kDa single transmembrane spanning glycoproteins that function as receptors for axonal guidance factors belonging to the class 3 semaphorin (Sema3) subfamily. The SemaA subfamily includes Sema3A and Sema3F (68-71) and members of the vascular endothelial growth factor (VEGF) family. *In vitro* results have demonstrated that Nrps bind to VEGF members in isoform-specific manners. Nrp-1 binds VEGF-A165, VEGF-B, VEGF-E, and placental growth factor (PLGF), whereas Nrp-2 binds VEGF-A145, VEGF-A165, VEGF-C, and PLGF (72).

Previously, Nrp-2 was identified as a component protein of the Sema3F receptor, which induces the repulsion of Nrp-2-expressing neuronal growth cones in the peripheral nervous system (68, 69, 73). Nrp-1 serves as a receptor for Sema3A, which induces neuronal growth cone collapse (74, 75).

Nrp-1 and Nrp-2 are found at synaptic sites. Nrp-1 is localized presynaptically, and Nrp-2 is localized postsynaptically (76).

Furthermore, a recent study showed that Nrp-2 is a receptor for secreted semaphorins (particularly Sema3F) that regulates the formation of synaptic spines and affects synaptic transmission (73).

Alzheimer’s disease

AD is the most common cause of dementia. The term AD originated in 1906 when Dr. Alois Alzheimer presented a case history of a 51-year-old woman who suffered from a rare brain disorder to a medical meeting. The autopsy of this patient identified the senile plaques and neurofibrillary tangles (NFTs) in the brain that currently characterize AD.

AD is well known as a progressive, neurodegenerative disorder that attacks the brain's neurons and results in behavioral changes and the loss of memory, thinking and language skills. Other cognitive and behavioral impairments include depression, delusions, hallucinations, anxiety, sexual disinhibition and aggression (77). Early studies identified an association between synaptic loss and cognitive impairment in AD patients (78). Neuropathologically, two types of abnormal lesions are present in the brains of subjects with AD: 1) senile plaques (including those caused by the abnormal processing of APP) that are primarily composed of the Aβ peptide that is generated by the proteolytic cleavage of APP by β-site APP cleaving enzyme-1 (BACE-1) and γ-secretase; and 2) NFTs, which are insoluble twisted fibers that build up inside neurons and are largely composed of the microtubule-stabilizing protein tau (NFT accumulation is due to the hyperphosphorylation of tau). The formation of senile plaques and NFTs is thought to contribute to the degeneration of the neurons in the brain and to the subsequent symptoms of AD.

In AD, there is an overall shrinkage of brain tissue. Additionally, the ventricles within the brain that contain the cerebrospinal fluid (CSF) are noticeably enlarged. In the early stages of AD, short-term memory begins to

fade as the cells in the hippocampus degenerate. The ability to perform routine tasks also declines. As AD spreads through the cerebral cortex (the outer layer of the brain), judgment declines and emotional outbursts and language impairment may occur. As the disease progresses, more neurons die, which leads to changes in behavior that can include wandering and agitation. In the final stages of the disease, patients may lose the abilities to recognize the faces of others and communicate, and patients typically cannot control their bodily functions and require constant care.

AD has been suggested to be a form of neuroplastic failure (56, 79). Consistent with this suggestion, the potential for neuroplasticity in the adult varies across regions, and the potentials for synaptic plasticity, axonal and dendritic remodeling and synaptogenesis are particularly high in the areas that are affected early in AD (80). For example, plasticity-related increases in the length and branching of dendritic trees during adulthood (81), the expression of growth-associated protein 43 (GAP 43, which is a marker of axonal sprouting) (82) and the expression levels of the mRNAs for BDNF and TrkB receptors (83) are all relatively high in the hippocampus and entorhinal cortex. These findings indicate that the processes underlying experience-dependent remodeling and synaptic turnover in the adult brain are particularly vulnerable to the primary causes of AD.

The Aβ hypothesis of AD proposes that Aβ is a primary cause of the disease (84). APP is transported along the axon to the presynaptic axon terminal where it is incorporated into the membrane. APP is a protein with a large extracellular amino terminus and a short cytoplasmic C-terminus. Aβ is a 4-

kDa peptide of 39-43 amino acids that is located within a section of the APP that spans the transmembrane domain; Aβ resides partly outside and partly within the membrane (85, 86). APP is cleaved by two distinct pathways; i.e., the non-amyloidogenic and amyloidogenic pathways. In the non-amyloidogenic pathway, APP is cleaved between the C-terminal side of residue 16 and 17 of Aβ by α-secretase to yield a secreted form of APP termed sAPPα (which is a large 90-kDa N-terminal portion) and an 83-amino acid C-terminal fragment (C83)(87). The activity of α-secretase is associated with several members of the disintegrin and metalloproteinase (ADAM) family that include ADAM9, ADAM10 and ADAM17. APP processing via the amyloidogenic pathway results in an approximately 99-amino acid transmembrane fragment termed C99 due to proteolytic cleavage by β-secretase at the N-terminal site (88). C99 is further cleaved inside the membrane by γ-secretase (which includes presenilin-1, nicastrin, APH-1 and PEN-2) to yield the APP intracellular domain, which is a fragment with a putative nuclear signaling role, and Aβ (predominantly $A\beta_{1-40}$ and $A\beta_{1-42}$). The $A\beta_{1-40}$ and $A\beta_{1-42}$ species of Aβ are highly hydrophobic and have been specifically implicated in causing AD (89).

Epidemiological data recently extracted from Latin American countries indicate that the prevalence of dementia is strongly age-dependent and increases exponentially among people over the age of 80 years (90). These findings were accompanied by figures that indicate that the prevalence of AD, which affected 26.6 million people worldwide in 2006 (91), will quadruple by 2050.

CHAPTER 1

Role of miR-188 in dendritic plasticity

INTRODUCTION

Many miRNAs and their precursors, along with the components of the miRNA machinery, exist in synaptic fractions (92), where they are poised to regulate neurotransmission. LTP is a cellular model that mimics long-term memory, requiring protein synthesis (93). The structural changes in synaptic connectivity that follow the physiological changes in synaptic strength must involve the gene regulatory networks that control synaptic development, maturation and maintenance. miRNAs rapidly and coordinately regulate the stability and translation of sets of mRNAs that mediate specific processes (94, 95), suggesting that miRNAs could possess an important role in homeostatic synaptic plasticity (96). Despite considerable evidence for the regulatory functions of miRNAs, the identities of the miRNA species that are involved in the regulation of synaptic transmission and plasticity as well as the mechanisms by which these miRNAs exert their functional roles remain largely unknown.

In this study, I investigated the roles and the regulatory mechanisms of miRNAs in the hippocampus during LTP. Through microarray analysis of miRNAs, I found that the expression levels of several miRNAs, including miR-188 were upregulated in rat hippocampal slices after LTP induction. The target molecules of miR-188 were, in turn, sought bioinformatically by employing miRNA-target gene prediction algorithms. Nrp-2 has a conserved binding site for miR-188 in its 3'-UTR (positions 163-183 of the rat 3'-UTR). Therefore, I found that miR-188 directly regulates the protein expression of

Nrp-2, which is a negative regulator for dendritic spine density in the CNS (73). In addition, I showed that Nrp-2 overexpression diminished dendritic spine densities, but miR-188 rescued this reduction.

MATERIALS AND METHODS

1. Hippocampal slice preparation and LTP induction

All *in vivo* experiments were performed in accordance with 'the Guidelines for Animal Experiments set forth by the Ethics Committee of Seoul National University'. Acute hippocampal slices were prepared from 4- to 5- week-old (90~110 g) male Sprague-Dawley (SD) rat brains. Briefly, brains were rapidly removed and coronal brain slices (400 μm) containing hippocampus, were cut on a Vibratome (Leica, Germany) in ice-cold aCSF [119 mM NaCl, 2.5 mM KCl, 1 mM $MgSO_4$, 2.5 mM $CaCl_2$, 1.25 mM NaH_2PO_4, 26 mM $NaHCO_3$ and 10 mM glucose] that was bubbled with 95 % O_2/5 % CO_2 to adjust to pH 7.4. After 1.5 h recovery at 27℃, an individual slice was transferred to a submerged recording chamber and continuously superfused with oxygenated aCSF at a rate of 2.5-3 ml/min at 33 ± 1℃.

LTP was introduced by changing the bath solution to Mg^{2+}-free aCSF solution containing 1 mM glycine, 1 μM strychinine (Sigma-Aldrich, MO, USA) and 100 μM picrotoxin (PTX) (119 mM NaCl, 2.5 mM KCl, 1.25 mM NaH_2PO_4, 26 mM $NaHCO_3$, 10 mM Glucose, 2.5 mM $CaCl_2$, pH 7.4) for 15 min as previously described (97), then recorded in basal bath solution for 2 h.

2. MicroRNA microarray analysis

The synthesis of target miRNA probes and hybridization were performed using Agilent's miRNA Labeling Reagent and Hybridization kit (Agilent Technology, CA, USA) according to the manufacturer's instructions. Briefly,

each 100 ng of total RNA (including small RNA fraction) was dephosphorylated with ~15 Units of calf intestine alkaline phosphatase, followed by RNA denaturation with ~40 % anhydrous dimethyl sulfoxide (DMSO, Duchefa, USA) and 10 min incubation at 100℃. Dephosphorylated RNA were ligated with pCp-Cy3 mononucleotide and purified with MicroBioSpin 6 columns (Bio-Rad, CA, USA). After purification, labeled samples were re-suspended with Gene Expression blocking Reagent and Hi-RPM Hybridization buffer, followed by boiling for 5 min at 100℃ and chilled for 5 min on ice. Finally, denatured labeled probes were pipetted onto assembled Agilent's miRNA Microarray (15K) and hybridized for 20 h at 55℃ with 20 RPM rotating in an Agilent Hybridization oven (Agilent Technology, CA, USA). The hybridized microarrays were washed as described in the manufacturer's washing protocol (Agilent Technology, CA, USA).

3. Data acquisition and analysis

The hybridized images were scanned using Agilent's DNA microarray scanner and quantified with Feature Extraction Software (Agilent Technology, CA, USA). All data normalization and selection of fold-changed genes were performed using GeneSpringGX 7.3 (Agilent Technology, CA, USA). The averages of normalized ratios were calculated by dividing the average of the normalized signal channel intensity by the average of normalized control channel intensity. Functional annotation of genes was performed according to the Gene OntologyTM Consortium (www.geneontology.org/index.shtml) by

GeneSpringGX 7.3.

4. MicroRNA target prediction analysis

The target mRNAs of specific miRNAs were predicted by searching on public databases with prediction algorithms, such as MicroCosm (www.ebi.ac.uk/enright-srv/microcosm/htdocs/targets/v5/).

5. Cell culture

Human embryonic kidney 293 (HEK 293 cells) were maintained in Dulbecco's modified Eagle's medium (DMEM) containing 10 % FBS, 50 U/ml penicillin and 50 μg/ml streptomycin at 37℃ in a humidified environment of 95 % O_2/5 % CO_2. Rat primary hippocampal neuron cultures were prepared from the hippocampi of E18-19 pregnant SD rats by dissociation with 0.25 % trypsin and plating onto coverslips coated with poly-L-lysine. The neurons were grown in Neurobasal medium (Gibco, CA, USA) supplemented with B27 (Gibco, CA, USA), 2 mM GlutaMAX-I supplement (Gibco, CA, USA) and 100 μg/ml penicillin/streptomycin (Gibco, CA, USA) at 37℃ in a humidified environment of 95 % O_2/5 % CO_2.

6. DNA constructs

The Nrp-2 cDNA in the internal ribosome entry site (IRES)-mGFP vector was a generous gift from Dr. Kolodkin. The 3'-UTR of the rat Nrp-2 mRNA (GenBank Accession No. NM_030869) was amplified by PCR from a rat brain cDNA library and subsequently inserted downstream of the Nrp-2 open

reading frame, which was confirmed by sequencing. For the luciferase activity assay, the 3'-UTR of the rat Nrp2 mRNA was amplified by PCR and then subcloned into the SpeI / MluI cloning site located downstream of the firefly luciferase gene in the pMIR-REPORT miRNA expression vector (Ambion, TX, USA). Point mutations were introduced into a possible miR-188 binding site located in the Nrp2 3'-UTR using an inverse PCR (iPCR)-based site-directed mutagenesis kit (KOD-Plus Mutagenesis Kit, Toyobo, Japan). The expression vectors for rno-miR-188 (miRBase Accession No. MI0006134) were prepared by introducing synthesized oligonucleotides corresponding to the mature miRNA sequences into the pLL3.7-DsRed2. All of the constructs were sequenced using an ABI310 Sequencer. The sequence of miR-188 mimic is 5'-CATCCCTTGCATGGTGGAGGG-3'; that of miR-SC is 5'-CCUCGUGCCGUUCCAUCAGGUAG-3'; that of miR-124 mimic is 5'-UAAGGCACGCGGUGAAUGCC-3' (synthesized based on the sequence of rno miR-124 (miRBase Accession No. MI0000828). The sequence of the antisense 2'-O-methyl (2'-O-Me) oligonucleotide for miR-188 (2'-O-Me-188-AS) is 5'-rGrCrUrCrGrCrCrCrUrCrCrArCrCrArUrGrCmAmAmGmGmGmAmUmGrUr GrArGrA-3' (r, RNA base; m, 2'-O-methyl base).

7. Luciferase activity assay

HEK293 cells seeded at 3×10^5 cells per 6-well plate were co-transfected with one of the following combinations using Lipofectamine 2000 (Invitrogen, CA, USA) : 1) wild-type 3'-UTR of Nrp-2 in pMIR-REPORT (wt 3'UTR of Nrp-2) alone; 2) wt 3'-UTR of Nrp-2 plus 40 nM miR-188 oligonucleotide; 3) wt 3'-

UTR of Nrp-2 plus 80 nM miR-188 oligonucleotide; 4) wt 3'-UTR of Nrp-2 plus miR-SC oligonucleotide; 5) mutant type 3'-UTR of Nrp-2 in pMIR-REPORT (mt 3'-UTR of Nrp-2) alone; 6) mt 3'-UTR of Nrp-2 plus 40 nM miR-188 oligonucleotide; 7) mt 3'UTR of Nrp-2 plus 80 nM miR-188 oligonucleotide; or 8) mt 3'-UTR of Nrp-2 plus miR-SC oligonucleotide. The luciferase activity assays were performed 48 h after transfection using the Luciferase Assay kit (Promega, WI, USA) and were measured with a Centro LB960 reader (Berthold Technologies, TN, USA). The β-galactosidase activity was measured to normalize the luciferase activity.

8. Quantitative real-time RT-PCR (RT-qPCR)

The total RNA including small RNA fraction was extracted, and 0.5 μg was processed for cDNA synthesis using oligo$(dT)_{20}$ primers and SuperScript III reverse transcriptase (Invitrogen, CA, USA). The cDNA was then amplified on the 7500 Fast Real-Time PCR system (Applied Biosystems, CA, USA), employing the ΔΔCt method with SYBR Green I (Roche, CA, USA). The primers used were as follows: Nrp-2 forward, 5'-AGGCTAACAATGATGCCACC-3'; Nrp-2 reverse, 5'-GCAACCAAAGAGCTCCAGTC-3'; GAPDH forward, 5'-ACCACCATGGAGAAGGCTGG-3'; GAPDH reverse, 5'-CTCAGTATAGCCCAGGATGC-3. To quantify the miRNA expression levels, SyBr Green miRNA assay-based RT-qPCR (GenoExplorer™ miRNA qRT-PCR Kit, GenoSensor Corp., AZ, USA) and (miScript PCR Starter Kit, Qiagen, CA, USA) was performed on a 7500 Fast Real-Time PCR system, using the ΔΔCt

method. ROX was utilized as an endogenous reference to standardize the miRNA expression levels. All of the data were calibrated by the universal reference data.

9. Dendritic spine density analysis

Rat primary hippocampal neuron cultures (DIV 10-12) were transfected with one of the following combinations : 1) IRES-mGFP control vector alone; 2) Nrp-2-IRES-mGFP vector alone; 3) Nrp-2-IRES-mGFP vector plus miR-188-IRES-DsRed plasmid; 4) Nrp-2-IRES-mGFP vector plus 100 nM miR-124 oligonucleotide (Genolution Pharmaceuticals, Seoul, Republic of Korea); 5) Nrp-2-IRES-mGFP vector plus 100 nM miR-SC (Genolution Pharmaceuticals, Seoul, Republic of Korea); 6) miR-188-IRES-DsRed plasmid alone; or 7) IRES-mGFP control vector plus 100 nM 2'-O-Me miR-188 AS (IDT, CA, USA). The number of dendritic spines was evaluated at DIV 18-20. The fluorescent images were acquired with an LSM 510 confocal microscope (Carl Zeiss, Jena, Germany), using the same settings for all of the samples. The spines were counted within the 50- to 100-μm segments on the secondary dendrites that extended at least 40-80 μm beyond the cell body (soma).

10. Western blotting

For the western blotting, 30-50 μg of protein was loaded onto denaturing 10-15 % sodium dodecyl sulfate-polyacrylamide gel electrophoresis (SDS-PAGE) and transferred to PVDF membranes (Millipore, MA, USA). Each membrane was then incubated in 5 % skim milk or 5 % bovine serum albumin for 1 h at room temperature followed by overnight incubation with appropriate primary

antibodies (Nrp-2, 1:2,000, Cell Signaling, MA, USA; GAPDH, 1:5,000, Santa Cruz, CA, USA). The membrane was then incubated for 1 h at room temperature with anti-rabbit or anti-mouse secondary antibodies conjugated with horse-radish peroxidase (HRP) (1:5,000, Invitrogen, CA, USA). The HRP signals were visualized using an enhanced chemiluminescent (ECL) substrate (Thermo Fisher Scientific, IL, USA).

11. Statistical analysis

The data are expressed as the means ± SEM values. A one-way ANOVA and independent T-test and non-parametric Kruskal-Wallis or Mann-Whitney test (PASW Statistics 18, IL, USA) were used for determining the statistical significance. The results were considered to be statistically significant if $p<0.05$.

RESULTS

Synaptic activity induced by LTP upregulates miR-188 expression

LTP was induced in acute hippocampal slices by treatment with 1 mM glycine, 1 μM strychnine (Sigma-Aldrich, MO, USA) and 100 μM PTX in Mg^{2+} free aCSF at 25℃, (Fig. 1-2A) to investigate the changes in miRNA expression profiles during LTP induction.

Next, miRNA microarray screening was carried out to investigate the changes in the miRNA expression profile during LTP induction. From the 287 screened miRNAs in the array chip containing two sets of independent experiments [each set consisted of control, LTP (0.5 h), LTP (1 h) and LTP (2 h)], I found that three miRNAs were significantly altered when assessed by microarray analysis (the cut-off value of up- or down-regulation was 1.5 fold) (Fig. 1-2B). I confirmed the results from the miRNA microarray analysis by performing RT-qPCR. miR-188 showed a steep increase at 1 h after LTP induction (LTP (1 h), 1.7510 ± 0.3045 fold, n=3 compared with the control (1 h); $^{*}p$=0.045781) (Fig. 1-2C). This result is consistent with previous reports showing the importance of protein synthesis during the induction stage of synaptic plasticity, especially within 1 h of LTP induction, as demonstrated by treatment with anisomycin, an inhibitor of protein synthesis (98, 99). When anisomycin was applied to brain slices or to primary neuron cultures following LTP induction by electrophysiological or chemical methods, the level of synaptic potentiation was obscured (100).

Hippocampal slice cultures should contain neurons as well as glial cells (101). To determine which cell type was producing the miR-188, I investigated the expression of miR-188 in primary hippocampal neuron cultures, astrocytes and microglia by RT-qPCR. As shown in Fig. 1-2D, miR-188 was expressed approximately four- to five-folds more in primary neurons, compared with astrocytes and microglia.

miR-188 decreases Nrp-2 protein levels, but not Nrp-2 mRNA levels

By using different miRNA-target prediction algorithms, including MicroCosm, I predicted a list of target genes for miR-188 (2-8 nucleotides). Based on this list of target genes, I focused on Nrp-2 as a molecular target for miR-188. The RT-qPCR results showed that the mRNA level of Nrp-2 was not significantly altered at any time point (Fig. 1-3A), but the Nrp-2 protein level was significantly decreased 2 h after LTP induction in rat hippocampal slices (0.3500 ± 0.0740, n=3; normalized value compared with the control; $^{***}p$=0.000679) (Figs. 1-3B, -3C). I examined the protein levels of ephrin A1, another possible target for miR-188. However, there were no significant changes in the ephrin A1 protein levels at any time point following LTP induction (data not shown).

Through the bioinformatics matching analysis, I predicted that the seed sequence of miR-188 (2-8 nts) binds to the conserved binding site, 5'-AGGGGAU-3' (positions 176-182 of the rat 3'-UTR) on the 3'-UTR of the Nrp-2 mRNA and affects Nrp-2 protein translation (Fig. 1-4A). A luciferase activity assay was performed 48 h after co-transfecting pMIR-Luc-3'-UTR

constructs containing either the target binding sequence of miR-188 in the wild-type (WT)3'-UTR of the Nrp-2 mRNA or a mutant sequence containing the sequence (5'-AGGCCAU-3') in the miR-188 binding site (Fig. 1-4B), together with 40 nM or 80 nM of miR-188 or miR-SC oligonucleotides, in HEK 293 cells. The relative luciferase activity was reduced in the cells co-transfected with the wild-type 3'-UTR of Nrp-2 plus miR-188 (76.2822 ± 1.2642 %, n=6, $^{**}p$=0.003579), compared with the cells transfected only with the wt 3'-UTR of Nrp-2 (Fig. 1-4C). However, in the cells co-transfected with the wt 3'-UTR of Nrp-2 plus miR-SC, no significant difference was observed in comparison to the cells transfected only with the wt 3'-UTR of Nrp-2 (109.9178 ± 7.0928 %, n=3, p=0.432768). In case of the mt 3'-UTR, co-transfection with either miR-188 or miR-SC did not affect the luciferase activity (Fig. 1-4C). This result indicates that miR-188 specifically binds to the 3'-UTR of Nrp-2 and represses the translation of luciferase.

Based on this, I concluded that miR-188 binds directly to the 3'-UTR of the Nrp-2 mRNA and decreases the Nrp-2 protein level by translational repression (Figs. 1-3A-3C and -4C).

miR-188 restores the Nrp-2 induced reduction in the dendritic spine density

The majority of the excitatory synapses in the mammalian CNS are formed on dendritic spines, and spine morphology and distribution are critical for synaptic transmission, synaptic integration and plasticity (43, 102). A previous study showed that the knock-out of Nrp-2 induces an increase in the dendritic

spine number and the mEPSC frequency, especially in dentate gyrus (DG) GCs and cortical layer V (73).

To examine the role of Nrp-2 and its regulation by miR-188 at the synapse, I first made the construct for miR-188 overexpression using lentiviral vector system (Figs. 1-5A and -5B).

Thus, I transfected Nrp-2 cDNA that contained the 3'-UTR subcloned into IRES-mGFP alone or together with miR-188, (in IRES-DsRed2), miR-124 oligonucleotide, miR-SC oligonucleotide into primary hippocampal neuron cultures at DIV 10-12 and analyzed the number of dendritic spines at DIV 18-20 (Figs. 1-6A-F). In addition, the number of dendritic spines in the neurons transfected with control vector plus 2'-O-Me-188-AS were also investigated (Fig. 1-6G). First, I investigated the effects of 2'-O-Me-188-AS on Nrp-2 protein levels 24 h after transfecting 2'-O-Me-188-AS into primary hippocampal neuron cultures at DIV 13. The Nrp-2 protein level was found to be increased by treatment with 2'-O-Me-188-AS (Fig. 1-6I), indicating that the translation of Nrp-2 is regulated by endogenous miR-188 in rat primary hippocampal neuron cultures. In addition, the protein level of Nrp-2 in cells co-transfected with miR-188 was found to be decreased compared with the level in cells transfected with Nrp-2 only, whereas there was no change observed when miR-SC was co-transfected with Nrp-2 (Fig. 1-6J).

Nrp-2 overexpression reduced the number of dendritic spines per 10 μm of dendrites by a significant 51.4 % (4.1708 ± 0.2292, n=12, $^{***}p$=4.57E-12) compared with the mGFP-transfected control (8.1074 ± 0.3505, n=9, Figs. 1-6B and -6H). However, co-transfection with Nrp-2 plus miR-188 rescued the

reduction in the number of dendritic spines induced by Nrp-2 (7.8778 ± 0.33497, n=9, p=0.637684) compared with the control (8.1074 ± 0.3505, n=9, Figs. 1-5C and -5H), indicating an important role for miR-188 in regulating dendritic spine density. I also confirmed that this reversal effect by miR-188 was specific by showing that co-transfection with miR-SC or miR-124 did not reverse the reduction in the number of dendritic spines induced by Nrp-2 (Figs. 1-6D, -6E and -6H).

When miR-188 was transfected alone, a significant change in the dendritic spine density was not observed (8.6028 ± 0.4247, n=6, p=0.364828) compared to the control (8.1074 ± 0.3505, n=9, Figs. 1-6F and -6H). Although this result was somewhat inconsistent with our expectations, it is possible that endogenous miR-188 already plays a sufficiently large role in regulating Nrp-2 expression in rat primary hippocampal neuron cultures such that the addition of miR-188 does not affect the number of dendritic spines. In addition, it might be possible that the down-stream molecules of the Nrp-2 signaling pathway in dendritic spine formation, which have not been elucidated to date, are regulated by miR-188 or by other miRNAs (miR-338* and miR-29a*) found to be induced by LTP in my study.

(A)

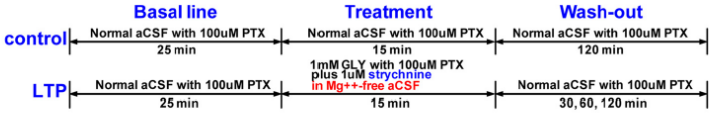
Basal line
Treatment
Wash-out
control
Normal aCSF with 100uM PTX
25 min
Normal aCSF with 100uM PTX
15 min
Normal aCSF with 100uM PTX
120 min
LTP
Normal aCSF with 100uM PTX
25 min
1mM GLY with 100uM PTX
plus 1uM strychnine
in Mg++-free aCSF
15 min
Normal aCSF with 100uM PTX
30, 60, 120 min

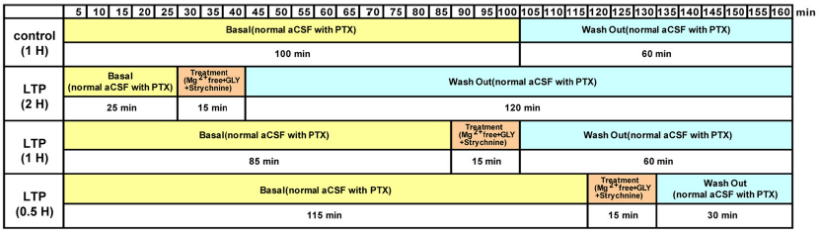
5 10 15 20 25 30 35 40 45 50 55 60 65 70 75 80 85 90 95 100 105 110 115 120 125 130 135 140 145 150 155 160 min
control (1 H)
Basal(normal aCSF with PTX)
Wash Out(normal aCSF with PTX)
100 min
60 min
LTP (2 H)
Basal (normal aCSF with PTX)
Treatment (Mg++free+GLY +Strychnine)
Wash Out(normal aCSF with PTX)
25 min
15 min
120 min
LTP (1 H)
Basal(normal aCSF with PTX)
Treatment (Mg++free+GLY +Strychnine)
Wash Out(normal aCSF with PTX)
85 min
15 min
60 min
LTP (0.5 H)
Basal(normal aCSF with PTX)
Treatment (Mg++free+GLY +Strychnine)
Wash Out (normal aCSF with PTX)
115 min
15 min
30 min

(B)

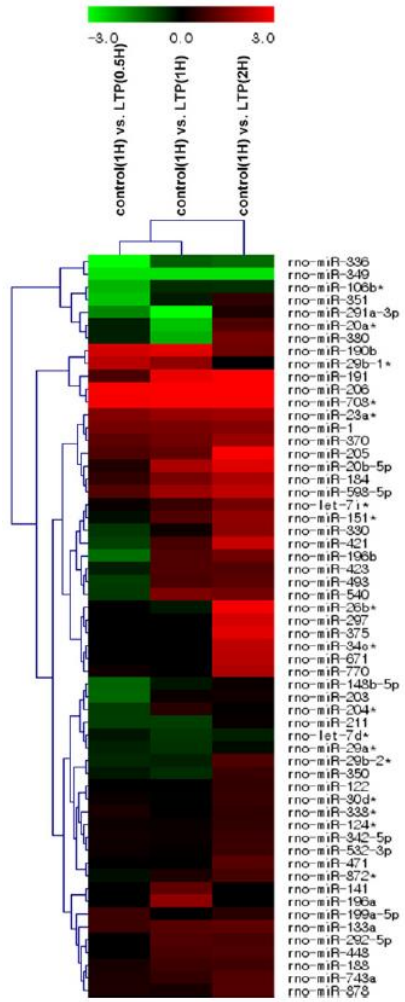
-3.0
0.0
3.0
control(1H) vs. LTP(0.5H)
control(1H) vs. LTP(1H)
control(1H) vs. LTP(2H)
rno-miR-336
rno-miR-349
rno-miR-106b*
rno-miR-351
rno-miR-291a-3p
rno-miR-20a*
rno-miR-380
rno-miR-190b
rno-miR-29b-1*
rno-miR-191
rno-miR-206
rno-miR-708*
rno-miR-23a*
rno-miR-1
rno-miR-370
rno-miR-205
rno-miR-20b-5p
rno-miR-184
rno-miR-598-5p
rno-let-7i*
rno-miR-151*
rno-miR-330
rno-miR-421
rno-miR-196b
rno-miR-423
rno-miR-493
rno-miR-540
rno-miR-26b*
rno-miR-297
rno-miR-375
rno-miR-34c*
rno-miR-671
rno-miR-770
rno-miR-148b-5p
rno-miR-203
rno-miR-204*
rno-miR-211
rno-let-7d*
rno-miR-29a*
rno-miR-29b-2*
rno-miR-350
rno-miR-122
rno-miR-30d*
rno-miR-338*
rno-miR-124*
rno-miR-342-5p
rno-miR-532-3p
rno-miR-471
rno-miR-872*
rno-miR-141
rno-miR-196a
rno-miR-199a-5p
rno-miR-133a
rno-miR-292-5p
rno-miR-448
rno-miR-188
rno-miR-743a
rno-miR-878

(C)

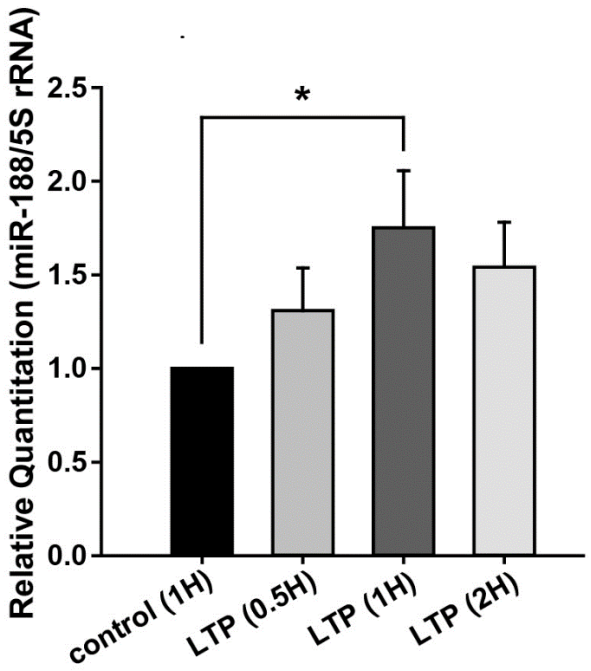
Relative Quantitation (miR-188/5S rRNA)
2.5
2.0
1.5
1.0
0.5
0.0
*
control (1H)
LTP (0.5H)
LTP (1H)
LTP (2H)

(D)

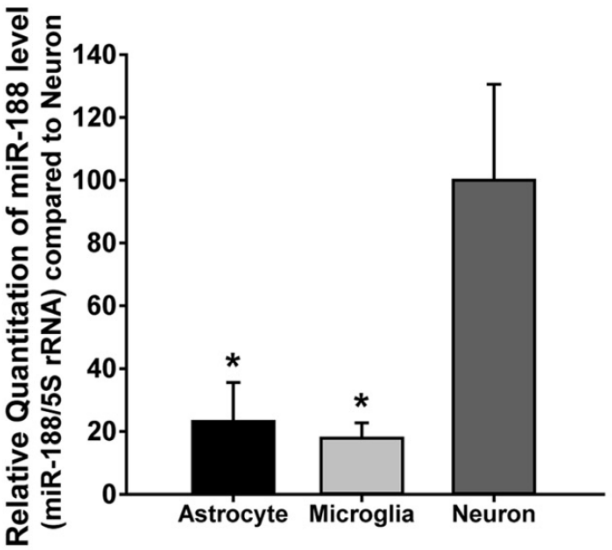
Relative Quantitation of miR-188 level
(miR-188/5S rRNA) compared to Neuron
140
120
100
80
60
40
20
0
*
*
Astrocyte
Microglia
Neuron

Figure 1-2. Synaptic activity upregulates miR-188 expression.

(A) The experimental scheme for LTP induction is shown. The time points for collecting hippocampal slices for RNA extraction are indicated (control, LTP-0.5 h, LTP-1 h, LTP-2 h). **(B)** Microarray screening of miRNAs was conducted to investigate the changes in miRNA expression during LTP using an array chip with 2 sets of independent experiment [each set consisted of control (1 h), chem-LTP (0.5 h), chem-LTP (1 h), chem-LTP (2 h)] (the cut-off value of up- or down-regulation is 1.5-fold) at different time points. A heat-map is shown. **(C)** RT-qPCR was performed to examine miR-188 in the rat hippocampal slices after LTP induction. The statistical analysis used a one-way ANOVA with LSD's *post hoc* test; the data are represented by the means ± SEM. **(D)** RT-qPCR was performed to examine miR-188 expression in primary hippocampal neuron cultures, astrocytes and microglia. The statistical analysis was performed using a one-way ANOVA with LSD's *post hoc* test; the data are represented by the means ± SEM.

(A)

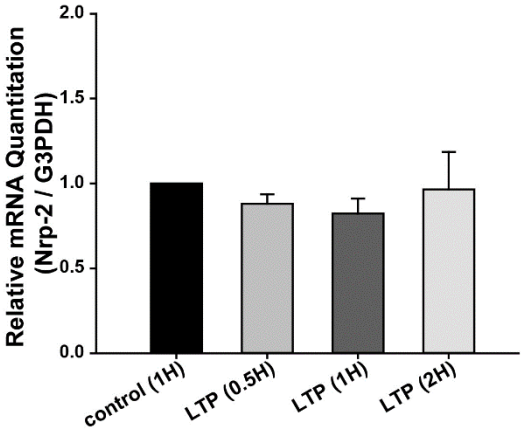
Relative mRNA Quantitation
(Nrp-2 / G3PDH)
2.0
1.5
1.0
0.5
0.0
control (1H)
LTP (0.5H)
LTP (1H)
LTP (2H)

(B)

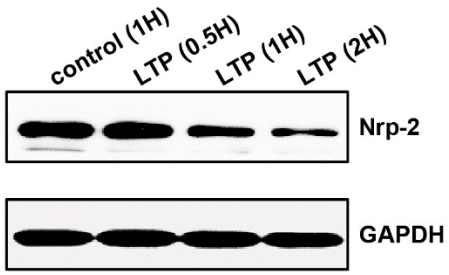
control (1H)
LTP (0.5H)
LTP (1H)
LTP (2H)
Nrp-2
GAPDH

(C)

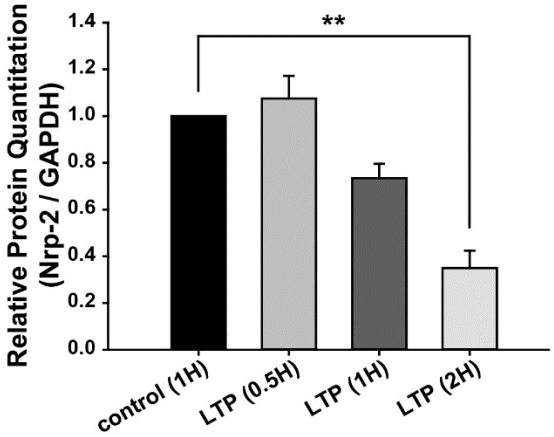
Relative Protein Quantitation
(Nrp-2 / GAPDH)
**
1.4
1.2
1.0
0.8
0.6
0.4
0.2
0.0
control (1H)
LTP (0.5H)
LTP (1H)
LTP (2H)

Figure 1-3. miR-188 decreases Nrp-2 protein levels, but not Nrp-2 mRNA levels.

(**A**) The mRNA level of Nrp-2 was examined in rat hippocampal slices by RT-PCR after LTP induction. **(B)** The Nrp-2 protein level was checked by western blotting with rat hippocampal slices after LTP induction. GAPDH served as the loading control. The blot is the representative of the three independent experiments. **(C)** The relative densitometrical value of Nrp-2 is shown in the graph. The statistical analysis was performed by a one-way ANOVA with Bonferroni's *post hoc* test; the data are represented by means ± SEM.

(A)

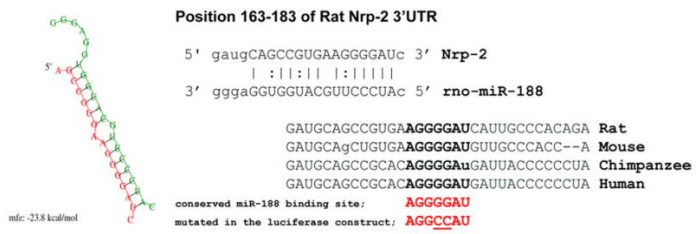
Position 163-183 of Rat Nrp-2 3'UTR
5' gaugCAGCCGUGAAGGGGAUc 3' Nrp-2
3' gggaGGUGGUACGUUCCCUAc 5' rno-miR-188
GAUGCAGCCGUGAAGGGGAUCAUUGCCCACAGA Rat
GAUGCAgCUGUGAAGGGGAUGUUGCCCACC--A Mouse
GAUGCAGCCGCACAGGGGAuGAUUACCCCCCUA Chimpanzee
GAUGCAGCCGCACAGGGGAUGAUUACCCCCCUA Human
conserved miR-188 binding site; AGGGGAU
mutated in the luciferase construct; AGGCCAU
mfe: -23.8 kcal/mol

(B)

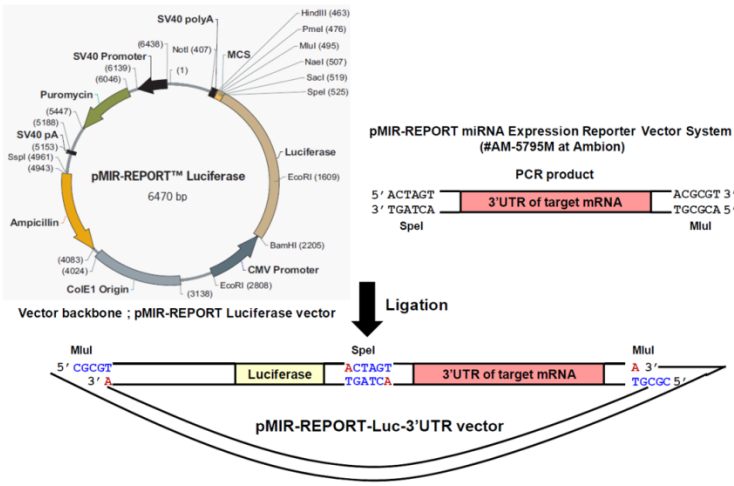
SV40 polyA
HindIII (463)
PmeI (476)
MluI (495)
NaeI (507)
SacI (519)
SpeI (525)
(6438)
NotI (407)
MCS
SV40 Promoter
(6139)
(6046)
(1)
Puromycin
(5447)
(5188)
SV40 pA
(5153)
SspI (4961)
(4943)
Luciferase
pMIR-REPORT™ Luciferase
6470 bp
EcoRI (1609)
Ampicillin
(4083)
(4024)
BamHI (2205)
CMV Promoter
ColE1 Origin
EcoRI (2808)
(3138)
Vector backbone ; pMIR-REPORT Luciferase vector
pMIR-REPORT miRNA Expression Reporter Vector System
(#AM-5795M at Ambion)
PCR product
5' ACTAGT
3' TGATCA
SpeI
3'UTR of target mRNA
ACGCGT 3'
TGCGCA 5'
MluI
Ligation
MluI
SpeI
MluI
5' CGCGT
3' A
Luciferase
ACTAGT
TGATCA
3'UTR of target mRNA
A 3'
TGCGC 5'
pMIR-REPORT-Luc-3'UTR vector

(C)

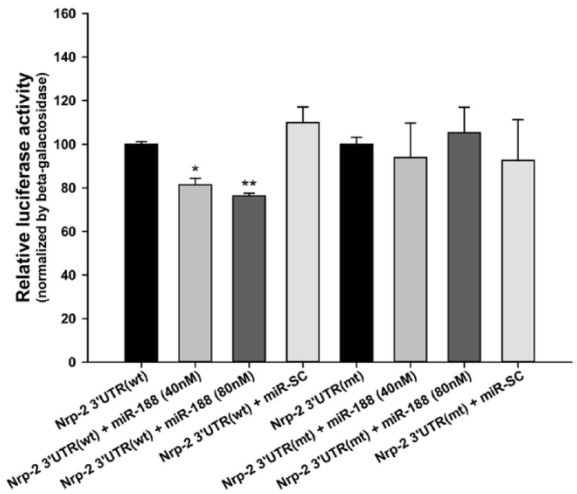
Relative luciferase activity
(normalized by beta-galactosidase)
160
140
120
100
80
60
40
20
0
*
**
Nrp-2 3'UTR(wt)
Nrp-2 3'UTR(wt) + miR-188 (40nM)
Nrp-2 3'UTR(wt) + miR-188 (80nM)
Nrp-2 3'UTR(wt) + miR-SC
Nrp-2 3'UTR(mt)
Nrp-2 3'UTR(mt) + miR-188 (40nM)
Nrp-2 3'UTR(mt) + miR-188 (80nM)
Nrp-2 3'UTR(mt) + miR-SC

Figure 1-4. Nrp-2 is a target for miR-188.

(**A**) The predicted hybridization of miRNAs (green) and the Nrp-2 (red) transcript using the RNAhybrid algorithm. The minimum free energy required for the hybridization is indicated. Right, a schematic diagram of rat Nrp-2 mRNA containing the predicted conserved target site of miR-188. (**B**) Schematic diagram of construct strategy for reporter assay. A PCR product of full length 3'-UTR of target mRNA was inserted into multiple cloning site (MCS) on pMIR-REPORT-Luc vector. (**C**) HEK 293 cells were co-transfected with one of the following combinations using Lipofectamine 2000 (Invitrogen, CA, USA) : 1) wild-type 3'-UTR of Nrp-2 in pMIR-REPORT (wt 3'UTR of Nrp-2) alone; 2) wt 3'-UTR of Nrp-2 plus 40 nM miR-188 oligonucleotide; 3) wt 3'-UTR of Nrp-2 plus 80 nM miR-188 oligonucleotide; 4) wt 3'-UTR of Nrp-2 plus miR-SC oligonucleotide; 5) mutant type 3'-UTR of Nrp-2 in pMIR-REPORT (mt 3'-UTR of Nrp-2) alone; 6) mt 3'-UTR of Nrp-2 plus 40 nM miR-188 oligonucleotide; 7) mt 3'UTR of Nrp-2 plus 80 nM miR-188 oligonucleotide; or 8) mt 3'-UTR of Nrp-2 plus miR-SC oligonucleotide. Luciferase activity assays were performed 48 h after transfection using the Luciferase Assay kit (Promega, WI, USA) and were measured with a Centro LB960 reader (Berthold Technologies, TN, USA). The β-galactosidase activity was measured to normalize the luciferase activity. The relative luciferase activity was reduced in the cells co-transfected with the wt 3'-UTR of Nrp-2 plus miR-188 (76.2822 ± 1.2642 %, n=6, $^{**}p$=0.003579), compared with the cells transfected only with the wt 3'-UTR of Nrp-2.

However, in the cells co-transfected with wt 3'-UTR of Nrp-2 plus miR-SC, no significant difference was observed in comparison to the cells transfected only with the wt 3'-UTR of Nrp-2. The statistical analysis was performed using a nonparametric Mann-Whitney for wt 3'-UTR of Nrp-2 and independent T-test for mt 3'-UTR of Nrp-2, respectively; the data are represented by the means ± SEM, respectively.

(A)

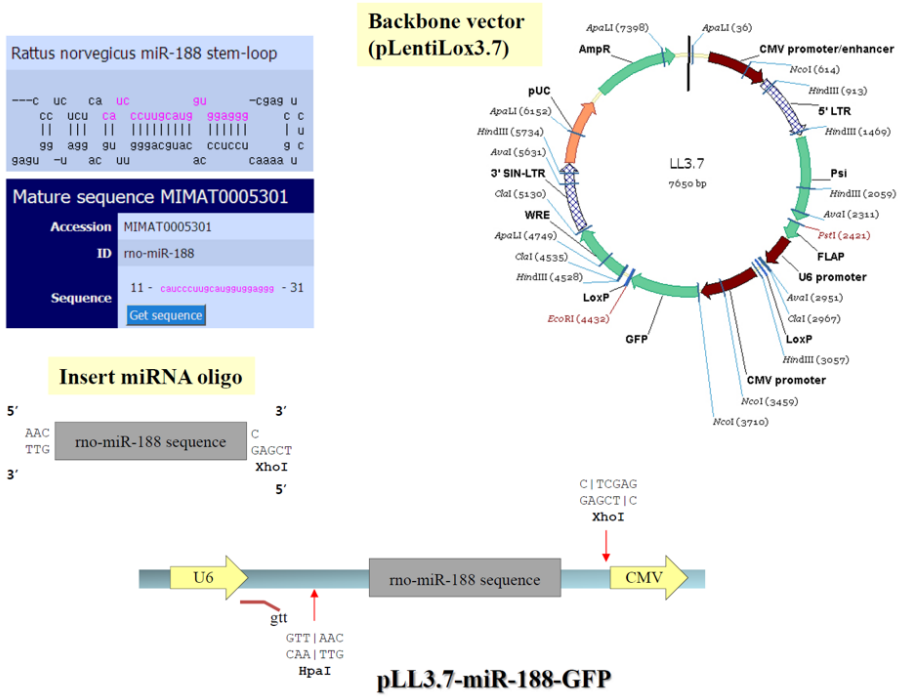
Rattus norvegicus miR-188 stem-loop
Mature sequence MIMAT0005301
Accession
MIMAT0005301
ID
rno-miR-188
Sequence
Get sequence
Backbone vector
(pLentiLox3.7)
LL3.7
7650 bp
AmpR
pUC
CMV promoter/enhancer
5' LTR
Psi
FLAP
U6 promoter
LoxP
CMV promoter
WRE
3' SIN-LTR
GFP
Insert miRNA oligo
rno-miR-188 sequence
XhoI
U6
CMV
gtt
HpaI
pLL3.7-miR-188-GFP

(B)

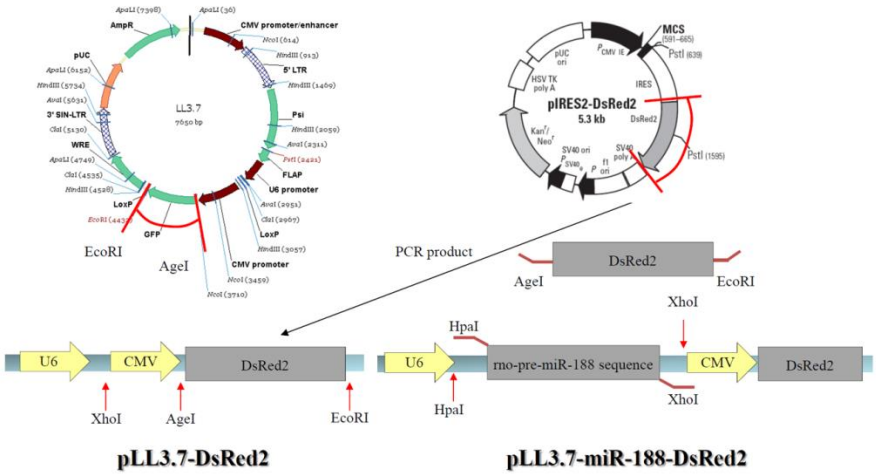
pIRES2-DsRed2
5.3 kb
MCS
IRES
DsRed2
PCR product
AgeI
EcoRI
XhoI
HpaI
U6
CMV
rno-pre-miR-188 sequence
pLL3.7-DsRed2
pLL3.7-miR-188-DsRed2

Figure 1-5. Construction strategy of miR-188 expression using lentiviral vector system

(**A**) Left, Schematic diagram of mature rno-miR-188 sequence (miRBase Accession No. MI0006134). Right, Map information of pLentiLox3.7 vector (103), which act as a backbone vector. Bottom, The lentiviral expression plasmids for miR-188 were constructed based on the Lentilox 3.7 plasmid (pLL3.7-miR-188-GFP). Sequences containing mature miRNAs were cloned into the HpaI/XhoI site of Lentilox 3.7. Lentivirus production was as described (104). (**B**) Schematic illustration for strategy of lentiviral miR-188-DsRed2 expression vector (pLL3.7-miR-188-DsRed2). The lentiviral expression plasmids for miR-188 were constructed based on modified the Lentilox 3.7 plasmid (pLL3.7-DsRed2).

(A) - (G)

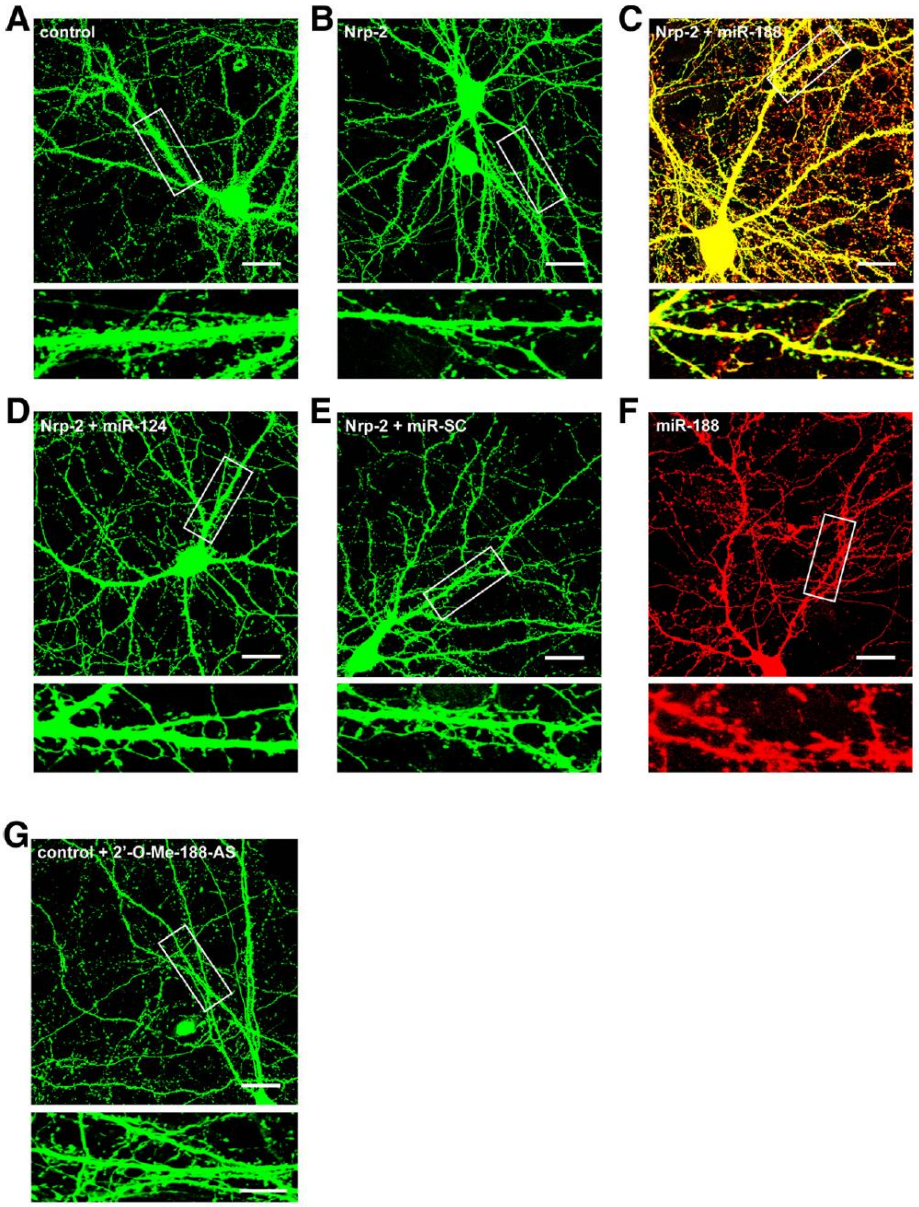
A
control
B
Nrp-2
C
Nrp-2 + miR-188
D
Nrp-2 + miR-124
E
Nrp-2 + miR-SC
F
miR-188
G
control + 2'-O-Me-188-AS

(H)

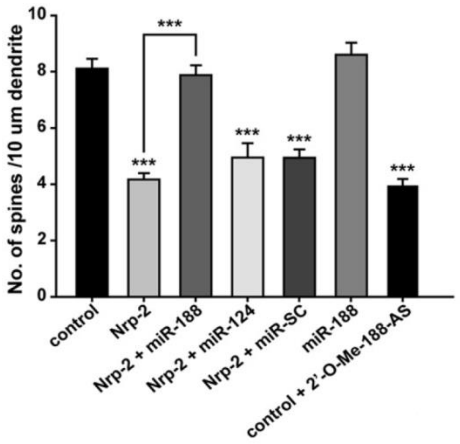
No. of spines /10 um dendrite
10
8
6
4
2
0
***
***
***
***
***
control
Nrp-2
Nrp-2 + miR-188
Nrp-2 + miR-124
Nrp-2 + miR-SC
miR-188
control + 2'-O-Me-188-AS

(I)

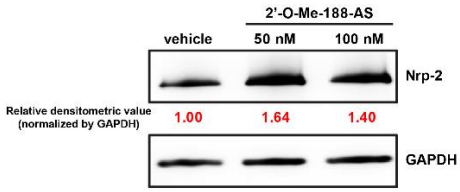
2'-O-Me-188-AS
vehicle
50 nM
100 nM
Nrp-2
Relative densitometric value
(normalized by GAPDH)
1.00
1.64
1.40
GAPDH

(J)

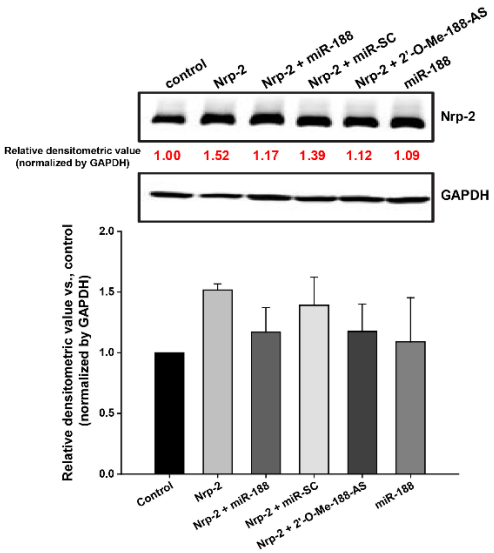
control
Nrp-2
Nrp-2 + miR-188
Nrp-2 + miR-SC
Nrp-2 + 2'-O-Me-188-AS
miR-188
Nrp-2
Relative densitometric value
(normalized by GAPDH)
1.00
1.52
1.17
1.39
1.12
1.09
GAPDH
Relative densitometric value vs., control
(normalized by GAPDH)
2.0
1.5
1.0
0.5
0.0
Control
Nrp-2
Nrp-2 + miR-188
Nrp-2 + miR-SC
Nrp-2 + 2'-O-Me-188-AS
miR-188

Figure 1-6. miR-188 reverses the Nrp-2-induced reduction in dendritic spine density.

(A) - (G) Representative images of dendritic spines on rat primary hippocampal neuron cultures at DIV 18-20 after transfecting Nrp-2 (in IRES-mGFP), either alone or with miR-188 (IRES-DsRed2), miR-124 or miR-SC oligonucleotides or transfecting with miR-188 alone or with IRES-mGFP vector plus 2'-O-Me-188-AS at DIV 10-12. The dendritic segment outlined with a white box (upper) is magnified to delineate spine morphology (bottom). The scale bars indicate 20 μm (low-scaled panel) and 5 μm (magnified panel). **(H)** A quantification of the spine density (40-80 μm of secondary dendritic spines from soma) in DIV 18-20 after transfection into primary hippocampal neuron cultures at DIV 10-12. Nrp-2 overexpression reduced the number of dendritic spines per 10 μm of dendrites by a significant 51.4 % (4.1708 ± 0.2292, n=12, $^{***}p$=4.58E-12) compared with the mGFP-transfected control (8.1074 ± 0.3505, n=9). Co-transfection with Nrp-2 plus miR-188 reversed the reduction in the number of dendritic spines induced by Nrp-2 (7.8778 ± 0.33497, n=9, p=0.637684) compared with the control (8.1074 ± 0.3505, n=9). However, co-transfection with miR-SC or miR-124 did not reverse the reduction in the number of dendritic spines induced by Nrp-2. The statistical analysis was performed by a one-way ANOVA with LSD's *post hoc* test; the data are represented by the means ± SEM. **(I)** The Nrp-2 protein level was assessed by western blotting after 2'-O-Me-188-AS (50 nM and 100 nM) treatment for 24 h in rat primary hippocampal neuron cultures. The blot is the

representative of the two independent experiments. The intensities of the bands were measured relative to the amount of GAPDH in each sample. The relative densitometric value vs. the vehicle -treated group is marked in numbers. **(J)** The Nrp-2 protein level was assessed by western blotting after transfection with Nrp-2 cDNA alone, or with Nrp-2 plus miR-188 or miR-SC or miR-188 alone in rat primary hippocampal neuron cultures. The blot is the representative of the three independent experiments. The intensity of the bands was measured relative to the amount of GAPDH in each sample. The relative densitometric value vs. the mGFP control group is shown in graph.

DISCUSSION

High abundance of miRNAs in the mammalian brain strongly suggests that miRNAs may represent important post-transcriptional regulators of gene expression by subtle but influential changes to the genetic programs that normally occur in neural cells (94, 105, 106). One miRNA can target up to several hundred genes (95, 107) to destabilize of mRNA transcripts that mediate complex cellular processes, such as development and plasticity, in a coordinated manner (96).

Synaptic plasticity is thought to underlie learning and memory, and LTP is a cellular model that mimics long-term memory and requires protein synthesis (93). Structural changes in synaptic connectivity that follow physiological changes in synaptic strength must involve gene regulatory networks controlling synaptic development, maturation and maintenance. miRNAs rapidly and coordinately regulate stability and translation of sets of mRNAs mediating specific processes (94, 95), suggesting that miRNAs could possess an important role in homeostatic synaptic plasticity (96). Despite considerable evidence for regulatory functions of miRNAs, it remains largely unknown which miRNA species are involved in regulation of synaptic transmission and synaptic plasticity and also how they exert functional roles (92).

In this study, I found that miR-188 expression was upregulated by LTP induction, and that it plays an important role in dendritic spine formation by specifically regulating the expression of Nrp-2. The 3'-UTR of Nrp-2 has possible binding sites for 29 miRNAs when predicted with MicroCosm

program. Among the 29 miRNAs, let-7a, let-7b, let-7c, miR-124, miR-126, miR-29b and miR-9 are known to be expressed in hippocampus. However, none of the 7 microRNAs showed significant changes in expression after LTP induction in our results with miRNA microarray analysis.

I confirmed that miR-188 expression was increased 1 h after LTP induction by performing RT-qPCR (Fig. 1-2C) and that Nrp-2 is a target for miR-188 by luciferase activity assay (Fig. 1-4C). miR-188 expression was detected to be increased 1 h after LTP induction and that a significant reduction in Nrp-2 was observed 2 h after LTP induction. This time difference is thought to be because that a certain amount of time is required for miR-188 to repress Nrp-2 protein translation.

Nrp-2 is a receptor for Sema3F, which is a negative regulator of spine development and synaptic structure. The Nrp-2 intracellular domain contains a C-terminal PDZ ligand motif that may be critical for Nrp-2/plexinA3 localization and Sema3F/ Nrp-2 is a receptor for Sema3F mediated regulation of spine morphology and synapse structure (73). Nrp-2 is enriched in the dentate gyrus molecular layer, where dendrites of granule cells reside. Sema3F is strongly expressed in the hilus, along the projection pathways of both the supra and intrapyramidal axons and the entorhinal cortex axons that innervate the dentate gyrus molecular layer. Therefore, Sema3F and Nrp-2 are expressed in patterns consistent with the hypothesis that these proteins direct postnatal hippocampal neural circuit formation (73). Mice with null mutations in genes encoding Sema3F and its holoreceptor Nrp-2 exhibit increased dentate gyrus granule cell and cortical layer V pyramidal neuron spine

number and size, as well as aberrant spine distribution. In contrast, a distinct Sema3A-Nrp-1/PlexA4 signaling cascade controls basal dendritic arborization in layer V cortical neurons but does not influence spine morphogenesis or distribution (73). During brain development, the growth cones of axons navigate towards the target field, where synapses are formed with the appropriate postsynaptic partner. It is becoming clear that pathfinding by most axons is dependent on a complex combination of secreted and membrane-bound cone attractants and repellents (108). Axons are guided by both positive and negative cues that they encounter as they find their way to their targets (109).

The VEGF family is involved in the formation of new blood vessels in both malignant and nonmalignant conditions, by binding with the Nrp-1 or -2 receptor in endothelial cells (74). However, the function of VEGF through these receptors in the CNS has not been defined, yet. Recently, it was reported that treatment with fluoxetine, an anti-depressant, induces VEGF expression in the brain and that this effect is related to antidepressant behaviors. VEGF was reported to be implicated in hippocampal neurogenesis in the rodent brain (110, 111). However, its exact mechanisms or action during LTP remains to be clarified. Nrp-2 may exert an effect on synaptic plasticity through other ligands such as VEGF together with Sema3F.

In addition, a recent report demonstrated that neuron-glial-related-cell adhesion molecule formed a molecular complex with Nrp-2 and the formation of this complex was required for growth cone collapse to Sema3F in thalamic neuron cultures (112).

In addition to the initially identified roles of miRNAs in development and cellular identity, more recently, their roles in neurodegenerative diseases have been appreciated (51, 53, 113).

Also, I found that the overexpression of miR-188 reversed the Nrp-2-induced reduction in dendritic spine density in primary hippocampal neuron cultures (Figs. 1-5A-G).

In conclusion, my study provides evidence that LTP induction causes time-dependent changes in miRNA expression, suggesting the involvement of these molecules in the cellular response to LTP.

CHAPTER 2

Pathophysiological role of miR-188 in Alzheimer's disease

INTRODUCTION

AD is a progressive neurodegenerative disease and is the most common cause of dementia among elderly people. AD results from multiple cellular and functional alterations in the brain. In AD, synaptic failures (79) that begin with subtle alterations in hippocampal synaptic efficacy occur prior to explicit neuronal degeneration, and the synaptic dysfunctions of AD are caused by diffusible oligomeric assemblies of the Aβ protein.

Recently, several studies have implicated miRNA dysregulations in the regulation of Aβ peptide (51, 53, 114-116) and tau (117, 118), inflammation (119-123), cell death (124, 125), and other aspects that compose the main pathomechanisms of AD. Additionally, miRNAs are differentially regulated in the blood (126, 127), and CSF (49, 128), and alterations in miRNA levels in these fluids may be indicative of AD. However, few miRNAs have been significantly linked to the pathophysiologies of synaptic dysfunction in AD.

In Chapter I, I investigated the roles and the regulatory mechanisms of miRNAs in the hippocampus during LTP and found that the expression levels of several miRNAs, including miR-188, were upregulated in rat hippocampal slices after the induction of LTP. These miRNAs function as positive regulators of dendritic spine plasticity via the downregulation of Nrp-2 expression (129).

In Chapter II, I investigated whether activity-dependent miR-188 was implicated in the pathogenesis of AD and whether this miRNA plays an important role in AD.

MATERIALS AND METHODS

1. Transgenic mice

Transgenic AD model mice with 5 x FAD mutations were purchased from Jackson Laboratories (strain: B6SJL-Tg [APPSwFlLon, PS1*M146L*L286V] 6799Vas/J) and maintained by crossing hemizygous transgenic mice with B6SJL F1 mice (130). Founder transgenic mice were identified by PCR, and non-transgenic littermate mice served as controls. 5 x FAD mice express both mutant human APP695 with the Swedish mutation (K670N, M671L), Florida mutation (I716V), and London mutation (V717I) and human presenilin 1 harboring two FAD mutations (M146L and L286V). Both transgenes are expressed under the control of the mouse Thy1 promoter to induce overexpression in the brain (130). These mice exhibit AD-related pathology earlier than other animal models, and amyloid deposition starts in the deep cortex and subiculum at 2 months of age. Synaptic marker proteins decrease at 4-9 months, and memory deficits are detected from 4-6 months of age (131). Importantly, amyloid plaques and neuronal death are not detected in the hippocampus at 4 months. Because I focused on the early events of AD pathology, before severe neurodegeneration has occurred, all animals in this study were killed after 4-8 months of age. Animal treatment and maintenance were performed in accordance with the Animal Care and Use Guidelines of Seoul National University, Seoul, Korea.

2. Oligomeric $A\beta_{1-42}$ preparation

Oligomeric $A\beta_{1-42}$ was prepared as described (132). Briefly, $A\beta_{1-42}$ peptide (American Peptides, Sunnyvale, CA, USA) was initially dissolved in 1,1,1,3,3,3-hexafluoro-2-propanol (HFIP; Sigma-Aldrich, St. Louis, MO, USA) to a concentration of 1 mg/ml. The peptide solution was divided into aliquots and the HFIP removed by evaporation under vacuum in a heated SpeedVac (Savant Instruments, Holbrook, NY). The dry peptide was stored at -70℃ until further processing. Before use, the $A\beta_{1-42}$ was dissolved in anhydrous DMSO (Duchefa, USA) to 1 mM, subsequently diluted to 5 μM, using F12 medium (Gibco/BRL, Grand Island, NY, USA) to indicated concentration. Most of Aβ forms are oligomers and some monomers exist in the mixture (133). For Aβ monomer preparation, Aβ in DMSO was diluted immediately to the appropriate concentration, using cell culture media. For soluble oligomers, Aβ was diluted to 5 μM, using F12 medium and then incubated for 24 h at 4℃. This solution is verified to be fibril-free by SDS-PAGE.

3. Primary hippocampal neuron culture

Rat primary hippocampal neuron cultures were prepared from the hippocampi of E18-19 pregnant SD rats by dissociation with 0.25 % trypsin and plating onto 18 mmΦ coverslips or 6-well coated with 1 mg/ml poly-L-lysine. The neurons were grown in Neurobasal medium (Invitrogen, CA, USA) supplemented with B27 (Invitrogen, CA, USA), 2 mM GlutaMAX-I supplement (Invitrogen, CA, USA) and 100 μg/ml penicillin/streptomycin (Invitrogen, CA, USA) at 37℃ in a humidified environment of 95 % O_2/5 %

CO_2.

4. DNA constructs

The IRES-mGFP vector was a generous gift from Dr. Kolodkin. The expression vectors for rno-miR-188 (miRBase Accession No. MI0006134) were prepared by introducing synthesized oligonucleotides corresponding to the mature miRNA sequences into the pLL3.7-DsRed2. All of the constructs were sequenced using sequencer. The sequence of miR-188 mimic is 5'-CATCCCTTGCATGGTGGAGGG-3'; that of miR-SC is 5'-CCUCGUGCCGUUCCAUCAGGUAG-3'; that of miR-124 mimic is 5'-UAAGGCACGCGGUGAAUGCC-3' (synthesized based on the sequence of rno miR-124 (miRBase Accession No. MI0000828). The sequence of 2'-O-Me-188-AS is 5'-rGrCrUrCrGrCrCrCrUrCrCrArCrCrArUrGrCmAmAmGmGmGmAmUmGrUrGrArGrA-3' (r, RNA base; m, 2'-O-methyl base).

5. RT-qPCR

The total RNA including small RNA fraction or only small RNA fraction was extracted by miRNeasy Mini kit (cat no. 217004, Qiagen, CA, USA) or NucleoSpin miRNA kit (cat no. 740971, Macherey-Nagel, Duren, Germany), and 0.5-1.0 μg was processed for cDNA synthesis using miScript PCR Starter Kit (cat no. 218193, Qiagen, CA, USA). The primers used were as follows: miR-188-5p (using cat no. 00001757, miScript Primer Assays, CA, USA), 5' CAUCCCUUGCAUGGUGGAGGG-3'; snRNA RNU6B (RNU6-2) provided

in miScript PCR Starter Kit. To quantify the miRNA expression levels, SYBR Green miRNA assay-based RT-qPCR (using miScript PCR Starter Kit) was performed on a 7500 Fast Real-Time PCR systems (Applied Biosystems, CA, USA), using the ΔΔCt method. ROX was utilized as an endogenous reference to standardize the miRNA expression levels. All of the data were normalized by the snRNA RNU6B or 5S rRNA.

6. Dendritic spine density analysis

Primary hippocampal neuron cultures (DIV 10-12) from wild-type and 5 x FAD P1 mice were transfected with one of the following combinations: 1) IRES-mGFP control vector alone; 2) IRES-mGFP control vector plus miR-188-IRES-DsRed plasmid. The number of dendritic spines was evaluated at DIV 18-20. The fluorescent images were acquired with an LSM 510 confocal microscope (Carl Zeiss, Jena, Germany), using the same settings for all of the samples. The dendritic spines were counted within the 50- to 100-μm segments on the secondary dendrites that extended at least 40-80 μm beyond the cell body (soma).

7. Western blotting

For the western blotting, 30-50 μg of protein lysed by RIPA buffer from whole cells or hippocampi was loaded onto denaturing 10-15 % SDS-PAGE gels and transferred to PVDF membranes (Millipore, MA, USA). Each membrane was then incubated in 5 % skim milk or 5 % bovine serum albumin for 1 h at room temperature followed by overnight incubation with

appropriate primary antibodies (Nrp-2, 1:2,000, Cell Signaling Technology; 6E10, 1:1,000, Covance; GAPDH, 1:5,000, Santa Cruz). The membrane was then incubated for 1 h at room temperature with anti-rabbit or anti-mouse secondary antibodies conjugated with HRP (1:5,000, Invitrogen, CA, USA). The HRP signals were visualized using an ECL substrate (Thermo Fisher Scientific, IL, USA).

8. Immunohistochemistry

The brains from human AD patients and age-matched control subjects in 10% neutral buffered formalin for 48 h were dehydrated and embedded in paraffin. Prior to immunostaining, slides were deparaffinized by oven heating and immersion in xylene. After dehydration through graded alcohols to water, a primary antibody was revealed by incubating the tissue slices for overnight against Nrp-2 (1:50, Cell Signaling Technology, MA, USA), followed by Alexa 488-conjugated secondary antibodies (1:100, Molecular Probes, Carlsbad, CA, USA). After three washes in permeabilization buffer and a wash in PBS, cells were mounted on microscope slides in mounting medium (DAKO, CA, USA). Confocal microscopic observation was performed using LSM 510 (Carl Zeiss, Jena, Germany).

9. Stereotaxic injection

miR-188 was stereotaxically injected as lentilox-miR-188-DsRed2- or DsRed2-lentivirus into the CA1 of bilateral hippocampus using a Kopf stereotaxic frame (Kopf Instruments, Tujunga, CA, USA). Lentivirus injected

into CA1 at 1.7 mm posterior to the bregma (AP), ±1.0 mm lateral to the midline (ML), 1.75 mm ventral to the surface of the skull (DV) at 6 months after birth. The injection ate was 0.22 ul / min for 4 min and retracted after 5 min.

10. Behavioral Test

Spontaneous alternation performance was tested using a T-maze, as described previously (134) (length of start and goal stems-30 cm, width-15 cm, height-7 cm and 7×7 cm center piece). A trial consisted of 2 runs, with a time interval of 2 min. After the mouse had been placed in the start arm, the animal was free to choose between both goal arms. Shortly after decision of goal arm, the goal arm was closed with the central partition, and the animal was confined in the chosen arm for 30 sec. The animal was then returned to his home cage. After thoroughly cleaning the T-maze with 70 % ethanol, the mice was put back to the start arm and was free to choose one of the goal arms. The main measure was the alteration ratio, defined as proportion of trials on which alternation occurred (first to the left arm and then to the right arm or vice versa), divided by the total amount of trials. Total of 4 trials were conducted over 2 days (2 trials per day).

Contextual fear conditioning was tested as described previously (135, 136). Each scrambler was connected to an electronic constant-current shock source that was controlled via an interface connected to a Windows 7 computer running EthoVision XT 8 software (Noldus Information Technology, VA, USA). A digital camera was mounted on the steel ceiling of each chamber,

and video signals were sent to the same computer for analysis. During training, mice were placed in the conditioning chamber (13 × 13 × 25 cm) for 3 min (for pre-shock) and then received three repetitions footshocks (0.7 mA, 2 s) at 1 min inter-trial intervals after habituation for 10 min in the same chamber on the day before training. On the next day, conditioned mice were placed in the same chamber, and the "freezing" time was measured over both period of 3 and 5 min. Conditioned freezing was defined as immobility except for respiratory movements. The total freezing time in the test period was represented as a percentage.

11. Statistical analysis

The data are represented as the means ± SEM values. Independent T-test and non-parametric Mann-Whitney test and a one-way ANOVA using *post hoc* (IBM SPSS Statistics 20, IL, USA) were used for determining the statistical significance. The results were considered to be statistically significant if $p<0.05$.

RESULTS

miR-188 is significantly downregulated in the cortices and hippocampi of AD patients

I performed RT-qPCR on samples from the brains from AD patients and age-matched control subjects to examine the expression level of miR-188 in AD patients compared to control subjects. miR-188 expression was significantly downregulated in the cerebral cortices (0.5434 ± 0.0737, n=5 vs. age-matched control subjects, 1.0000 ± 0.1873, n=3; $^{*}p$=0.013055) and hippocampi of AD patients (0.7358 ± 0.0533, n=6 vs. age-matched control subjects, 1.0000 ± 0.1117, n=4; $^{*}p$ =0.038048) (Fig. 2-1A and -1B). In the hippocampal regions of AD patients, Nrp-2 immunoreactivity was markedly increased relative to that of age-matched control subjects (100 ± 8.6590 %, n=3 in control group versus 318.0208 ± 10.8642%, n=3 in AD patient group, $^{***}p$=0.000096, Figs. 2-1C and -1D). However, Nrp-2 mRNA expression was not significantly different between subjects of these groups (cerebral cortices: 1.3823 ± 0.1661, n=3 vs. age-matched control subjects, 1.0000 ± 0.0971, n=3; p=0.067508; hippocampi: 0.7835 ± 0.0806, n=5 vs. age-matched control subjects, 1.0000 ± 0.0898, n=3; p=0.107254) (Fig. 2-1E); these findings suggest that miR-188 regulates Nrp-2 protein but not mRNA levels.

OA$\beta_{1\text{-}42}$ reduces the expression of miR-188 in primary hippocampal neuron cultures

To examine the effects of oAβ_{1-42} at the synapse, I first tested the oligomerization of synthetic Aβ_{1-42} peptide using western blotting (Fig. 2-2A). Next, I examined miR-188 expression and the Nrp-2 protein levels (the molecular target of miR-188) in rat primary hippocampal neuron cultures treated with 1- and 5-μM oAβ_{1-42}. Treatment with 5 μM oAβ_{1-42} for 24 h significantly decreased miR-188 expression (0.5242 ± 0.1276 vs. vehicle-treated group, n=11, $^{*}p$=0.034640), whereas treatment with 1 μM oAβ_{1-42} for 24 h did not affected miR-188 expression in rat primary hippocampal neuron cultures (0.9024 ± 0.2495 vs. vehicle-treated group, n=8, p=0.423901). Nrp-2 proteins levels were significantly increased by treatment with 5 μM oAβ_{1-42} for 24 h as revealed by western blot (Fig. 2-2C).

Based on these results, I hypothesize that the dysregulation of miR-188 expression in AD patients contributes to the synaptic dysfunction and ultimately to the cognitive impairments that are characteristic of the disease. AD is a devastating neurodegenerative disease that is characterized by progressive declines in memory and cognitive ability (137, 138). Neuronal cell death is thought to be the causative factor of AD; however, another possibility has emerged in which synaptic failure and impairments of cognitive function precede neuronal degeneration, particularly in the early phase of AD (79).

BDNF significantly increases miR-188 expression in rat primary hippocampal neuron cultures

Next, I examined whether treatment with BDNF affected miR-188 expression in rat primary hippocampal neuron cultures. BDNF is a neurotrophic factor that plays pivotal roles in synaptic plasticity and cognition (139, 140). Recently, it has been suggested that decreases in BDNF in the prefrontal cortex and hippocampus are related to the cognitive deficits observed in animal models of AD (141).

RT-qPCR analyses revealed that treatment with 20 ng/ml BDNF significantly upregulated miR-188 expression by approximately two-fold in rat primary hippocampal neuron cultures (2.5313 ± 0.5280 vs. vehicle-treated group, n=6, $^{*}p$=0.032497) (Fig. 2-2B). These results suggest that BDNF plays a fundamental role in miR-188 expression; however, the direct or indirect mechanism by which BDNF upregulates miR-188 requires further study.

miR-188 rescues the reduction in dendritic spine density induced by oA$\beta_{1\text{-}42}$ in rat primary hippocampal neuron cultures

The infusion of soluble Aβ oligomers into the CNS has been reported to selectively block LTP (142), acutely disrupt cognitive function (143, 144) and induce reductions in dendritic spine density that lead to synaptic loss (145, 146). Thus, I next investigated whether the treatment of DIV-17 rat primary hippocampal neuron cultures with 5 μM oA$\beta_{1\text{-}42}$ for 24 h would induce a significant reduction in dendritic spine density and whether this reduction could be reversed by the addition of mimic of miR-188. Confocal imaging analyses revealed that the treatment of the neurons with 5 μM oA$\beta_{1\text{-}42}$, resulting in a reduction in the number of dendritic spines compared to the

vehicle-treated control (3.5190 ± 0.4063, n=9 and 7.1957 ± 0.4355, n=10 for the 5 μM oAβ_{1-42}- and vehicle-treated control groups, respectively, $^{***}p$=0.000906) (Figs. 2-3A, -3C and -3H).

Consistent with my expectations, treatment with 20 ng/ml BDNF significantly increased dendritic spine density (9.0241 ± 0.5922, n=9, $^{*}p$=0.011369), compared to the vehicle-treated controls (Figs. 2-3A, -3D and -3H).

In contrast, the addition of the miR-188 mimic rescued the reduction in dendritic spine density that was induced by treatment with 5 μM oAβ_{1-42} (7.3485 ± 0.1768, n=9, p=0.750663) (Figs. 2-3A, -3E and -3H). Moreover, I confirmed that this reversal effect mediated by miR-188 was specific by demonstrating that cotransfection with miR-SC or miR-124 did not reverse the reduction in dendritic spine density that was induced by oAβ_{1-42} (3.5706 ± 0.1572, n=6, $^{***}p$=0.000007 for miR-124 with 5 μM oAβ_{1-42} treatment; 3.8923 ± 0.1458, n=8, $^{***}p$=0.000018 for miR-SC with 5 μM oAβ_{1-42} treatment) (Figs. 2-3A, -3F, -3G and -3H).

Based on this result, I conclude that the reduction in dendritic spine density was at least partially due to the decrease in miR-188 expression caused by oAβ_{1-42}.

miR-188 was significantly downregulated in the hippocampi of 5 x FAD mice compared to those of wild-type mice

I examined whether the expressions of miR-188 and its target Nrp-2 were altered in 5 x FAD mice relative to age-matched wild-type mice. RT-qPCR analyses confirmed that miR-188 was significantly downregulated in the

hippocampi of the 5 x FAD mice in an age-dependent manner (at PND1: 0.7661 ± 0.0321, n=11 vs. age-matched controls, 1.0000 ± 0.0944, n=7, $^{*}p$=0.027259; at 4 months of age: 0.7154 ± 0.1452, n=4 vs. age-matched controls, 1.0000 ± 0.0777, n=5, $^{*}p$=0.037743; at 6 months of age: 0.2811 ± 0.0327, n=3, vs. age-matched controls, 1.0000 ± 0.2654, n=4, $^{*}p$=0.013546) (Fig. 2-4A).

Dendritic spine density was reduced the primary hippocampal neuron cultures of 5 x FAD mice

To investigate whether dendritic spines were altered in the primary hippocampal neuron cultures of postnatal day 1 (PND1) 5 x FAD mice compared to wild-type mice, I evaluated the numbers of spines on the oblique dendrites in primary cultures of hippocampal neuron. The dendritic spine densities of the neurons from the 5 x FAD mice at DIV 18-20 were significantly reduced by 58.9% (4.0677 ± 0.1540 spines/10 μm, $^{***}p$=4.6444E-18) compared to the neurons of wild-type mice (6.9098 ± 0.1854 spines/10 μm) (Figs. 2-5A and -5B).

Viral-mediated expression of miR-188 in the hippocampus rescues the memory deficits of 5 x FAD mice

I examined whether the viral-mediated expression of miR-188 could ameliorate the deficits in hippocampus-dependent memory that are observed in 7-month-old 5 x FAD mice. I used spontaneous alternations in performance in a T-maze as indices of hippocampus-dependent spatial working memory.

Seven month-old 5 x FAD mice exhibited significant reductions in spontaneous alternation performance in the T-maze (42.5000 ± 5.3359, n=10) compared to the wild-type controls (67.8571 ± 7.1429, n=7; $^{*}p$=0.016265) (Fig. 2-6D). However, miR-188 overexpression did not rescue the impairments of spatial working memory that were observed in the 5 x FAD mice compared to control virus-infected 5 x FAD mice (Fig. 2-6D).

Next, I employed another hippocampus-dependent learning task (i.e., a contextual fear conditioning paradigm) in which mice learn to associate a distinct context with aversive footshocks (147). I found that the wild-type mice exhibited robust conditional fear responses as assessed by freezing when the mice were placed back into the conditioning chamber after training.

The percent of time spent freezing after the induction of contextual fear conditioning was significantly lower among the 5 x FAD mice (38.4815 ± 8.0372, n=9) compared to that of the wild-type mice (68.2667 ± 5.2255, n=10; $^{**}p$=0.003733). Moreover, the expression of miR-188 in the 5 x FAD mice significantly rescued freezing behavior (38.4815 ± 8.0372, n=9, $^{***}p$=0.000703) (Fig. 2-6E).

(A)

Name	NBB No.	Autopsy No.		Code	Storage	Sex	Age	Anatomical region	RNA conc.(ug/ul)
MFG-control#1	00-032	S00/059	100	K1	plastic bag -80℃	F	78	medial frontal gyrus	0.56104
MFG-control#2	99-100	S99/214	100	K1	plastic bag -80℃	M	79	medial frontal gyrus	0.99953
MFG-control#3	02-024	S02/055	300	GFM2	plastic bag -80℃	F	75	medial frontal gyrus	0.70519
MFG-AD #1	98-015	S98/028	234	A1	cryovial -80℃	F	87	medial frontal gyrus	0.617965
MFG-AD #2	00-091	S00/194	300	GFM2	plastic bag -80℃	F	76	medial frontal gyrus	0.313865
MFG-AD #3	00-054	S00/115	300	GFM1	plastic bag -80℃	M	59	medial frontal gyrus	0.38748
MFG-AD #4	03-017	S03/042	300	GFM2	plastic bag -80℃	M	67	medial frontal gyrus	0.713325
MFG-AD #5	04-068	S04/232	300	GFM2	plastic bag -80℃	F	72	medial frontal gyrus	0.72622
HPC-control#1	00-032	S00/059	100	D3	cryovial -80℃	F	78	hippocampus	0.78966
HPC-control#2	99-100	S99/214	100	D3	cryovial -80℃	M	79	hippocampus	0.50664
HPC-control#3	97-157	S97/368	100	K1	plastic bag -80℃	M	69	medial frontal gyrus	0.49711
HPC-control#4	95-078	S95/228	161	A1	cryovial -80℃	F	80	hippocampus	0.68976
HPC-control#5	02-024	S02/055	300	HIP2	cryovial -80℃	F	75	hippocampus	0.57379
HPC-AD #1	02-099	S02/307	300	GFM3	plastic bag -80℃	M	69	medial frontal gyrus	0.5492
HPC-AD #2	03-017	S03/042	300	HIP2	cryovial -80℃	M	67	hippocampus	0.83869
HPC-AD #3	98-132	S98/242	100	K1	plastic bag -80℃	M	75	medial frontal gyrus	0.40382
HPC-AD #4	00-038	S00/069	263	A	cryovial -80℃	F	82	hippocampus	0.54031
HPC-AD #5	03-016	S03/038	300	HIP3	cryovial -80℃	F	72	hippocampus	0.5221
HPC-AD #6	95-053	S95/131	157	E	cryovial -80℃	F	79	hippocampus	0.7476
HPC-AD #7	98-015	S98/028	234	B1	cryovial -80℃	F	87	hippocampus	1.02572
HPC-AD #8	04-068	S04/232	300	HIP3	cryovial -80℃	F	72	hippocampus	0.75664
HPC-AD #9	01-076	S01/173	300	HIP3	cryovial -80℃	M	75	hippocampus	0.37729
HPC-AD #10	01-095	S01/219	300	HIP3	cryovial -80℃	F	81	hippocampus	0.6166
HPC-AD #11	00-054	S00/115	300	HIP1	cryovial -80℃	M	59	hippocampus	0.44972

(B)

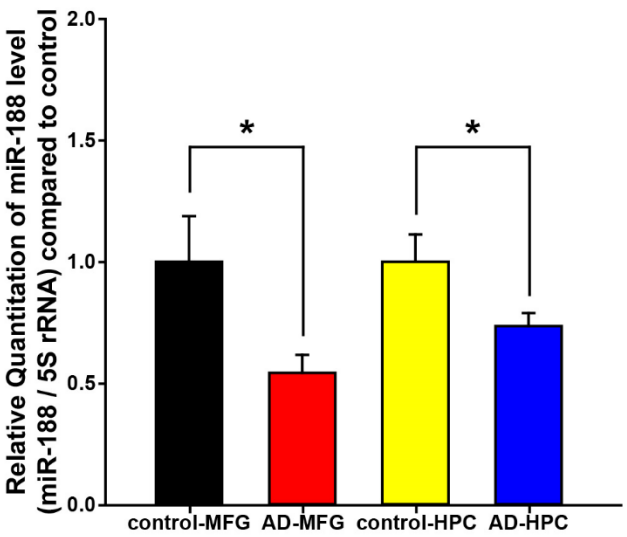

(C)

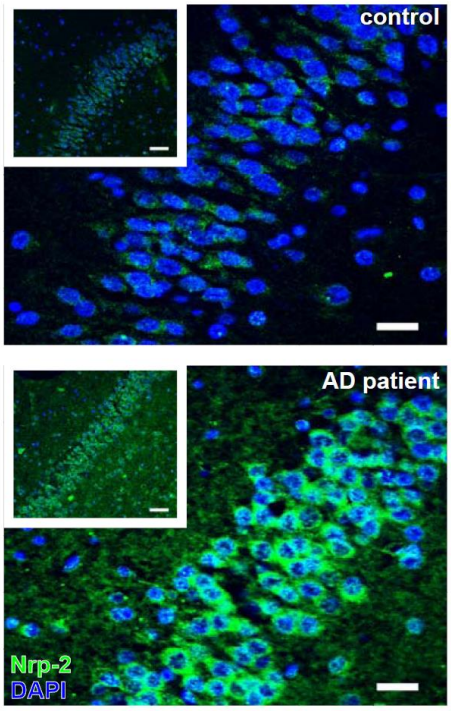
control
AD patient
Nrp-2
DAPI

(D)

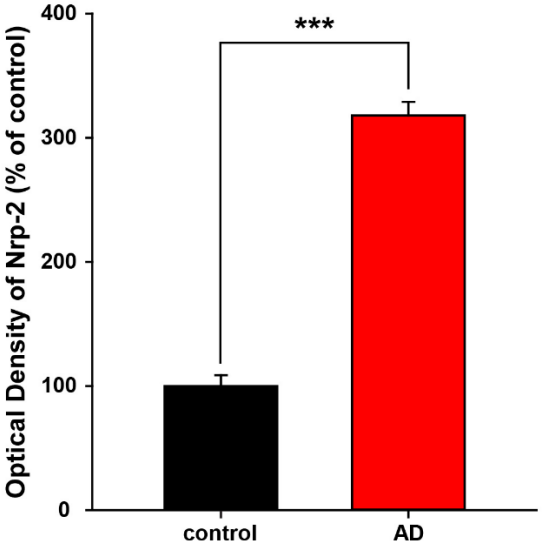
Optical Density of Nrp-2 (% of control)
400
300
200
100
0
***
control
AD

(E)

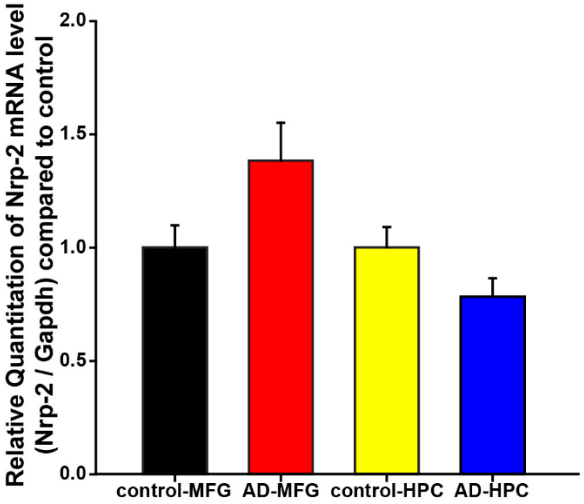

Figure 2-1. miR-188 is significantly downregulated in the cortices and hippocampi of AD patients.

(**A**) A representative table from the Human Sample Stock list for the medial frontal gyri (MFG) and the hippocampi (HPC) of human control and AD subjects. (**B**) The miR-188 expression levels were determined by RT-qPCR of the MFGs (the age-matched control subjects were 78, 79 and 75 years old, and the AD patients were 87, 76, 59, 67 and 72 years old) and HPCs of the human control and AD brains (the age-matched control subjects were 78, 79, 80 and 75 years old, and the AD patients were 72, 79, 87, 72, 81 and 59 years old). miR-188 expression was significantly downregulated in the cerebral cortices (0.5434 ± 0.0737, n=5 vs. age-matched control subjects, 1.0000 ± 0.1873, n=3; $^{*}p$=0.013055) and hippocampi (0.7358 ± 0.0533, n=6 vs. age-matched control subjects, 1.0000 ± 0.1117, n=4; $^{*}p$ =0.038048) of the AD

patients compared to the age-matched control subjects. 5S rRNA was used as an endogenous control. Statistical analyses were performed with independent t-tests for the MFG ($^{*}p$ <0.05) and with Mann-Whitney U tests for the HPC ($^{*}p$ <0.05). The error bars indicate the SEMs. **(C)** Representative images of the dentate gyrus of an AD patient (98 years old) and those of age-matched control subjects. Nrp-2 immunoreactivity was measured by immunohistochemistry. Scale bars indicate 50 μm (inset, white square box) and 20 μm (magnified panel). **(D)** Bar graphs depicting the Nrp-2 immunoreactivities of the AD patients and age-matched control subjects (100 ± 8.6590%, n=3 in the age-matched control group vs. 318.0208 ± 10.8642%, n=3 in the AD patient group, $^{***}p$=0.000096). $^{***}p$<0.001 indicates statistically significance differences between the control and AD patient groups by independent t-tests. **(E)** Bar graphs depicting Nrp-2 mRNA levels in the cerebral cortices (1.3823 ± 0.1661, n=3 vs. age-matched control subjects, 1.0000 ± 0.0971, n=3; p=0.067508) and hippocampi (0.7835 ± 0.0806, n=5 vs. age-matched control subjects, 1.0000 ± 0.0898, n=3; p=0.107254) of the AD patients and age-matched control subjects. $^{*}p$<0.05 indicates statistically significance differences between the control and AD patient groups by Mann-Whitney U tests for the MFG and by independent t-tests in the HPC.

(A)

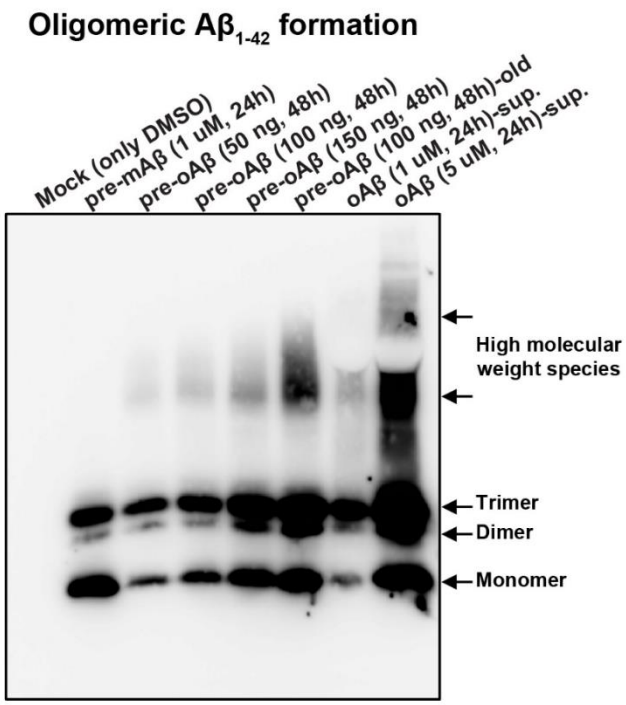
Oligomeric Aβ1-42 formation
Mock (only DMSO)
pre-mAβ (1 uM, 24h)
pre-oAβ (50 ng, 48h)
pre-oAβ (100 ng, 48h)
pre-oAβ (150 ng, 48h)
pre-oAβ (100 ng, 48h)-old
oAβ (1 uM, 24h)-sup.
oAβ (5 uM, 24h)-sup.
High molecular weight species
Trimer
Dimer
Monomer

(B)

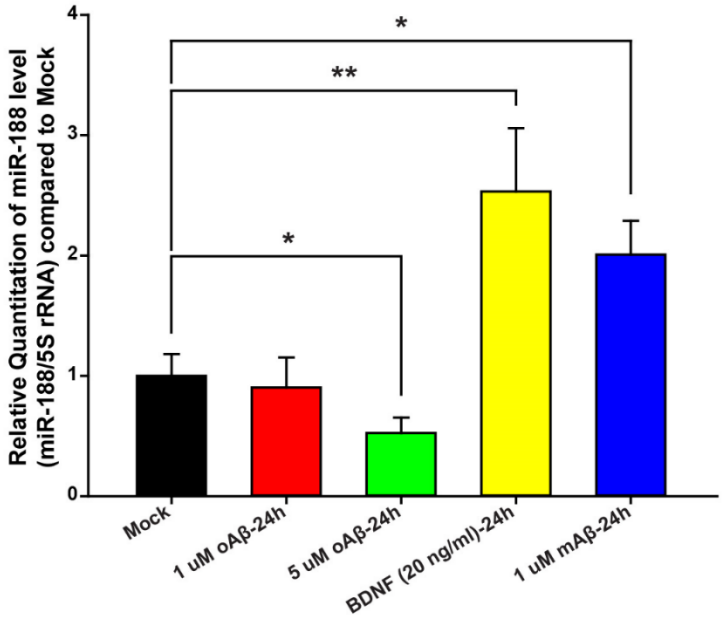
Relative Quantitation of miR-188 level (miR-188/5S rRNA) compared to Mock
0
1
2
3
4
*
**
*
Mock
1 uM oAβ-24h
5 uM oAβ-24h
BDNF (20 ng/ml)-24h
1 uM mAβ-24h

(C)

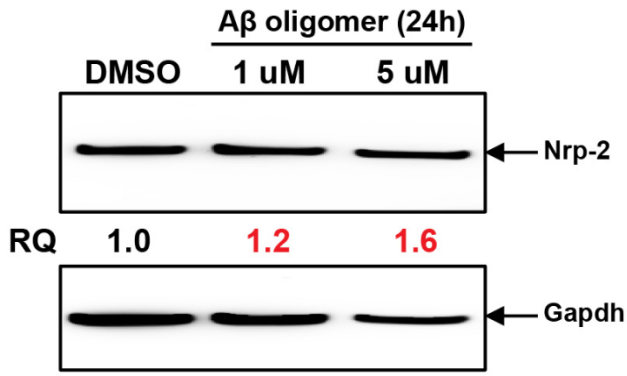

Figure 2-2. OAβ_{1-42} significantly increased the Nrp-2 protein levels.

(**A**) OAβ_{1-42} was generated by incubating Aβ_{1-42} monomers in serum-free F12 medium for 1 day at 4℃. Anti-Aβ western blot analyses revealed that this oligomeric preparation was enriched in dimer and trimer species. The dimers and trimers were present in monomer preparations. **(B)** miR-188 expression was examined by RT-qPCR after the treatment of primary hippocampal neuron cultures with oAβ_{1-42}. miR-188 expression was significantly reduced by treatment with 5 μM oAβ_{1-42} (0.5242 ± 0.1276, n=11) compared to the levels in the vehicle-treated control group (1.0000 ± 0.1819, n=10; $^{*}p$=0.034640 by Mann-Whitney U test). The data are presented as the means ± the SEM. **(C)** The Nrp-2 protein levels in the primary hippocampal neuron cultures after oAβ_{1-42} treatment were examined with immunoblotting (RQ, relative quantitation of the oAβ_{1-42} treatment compared to the control treatment).

(A) - (G)

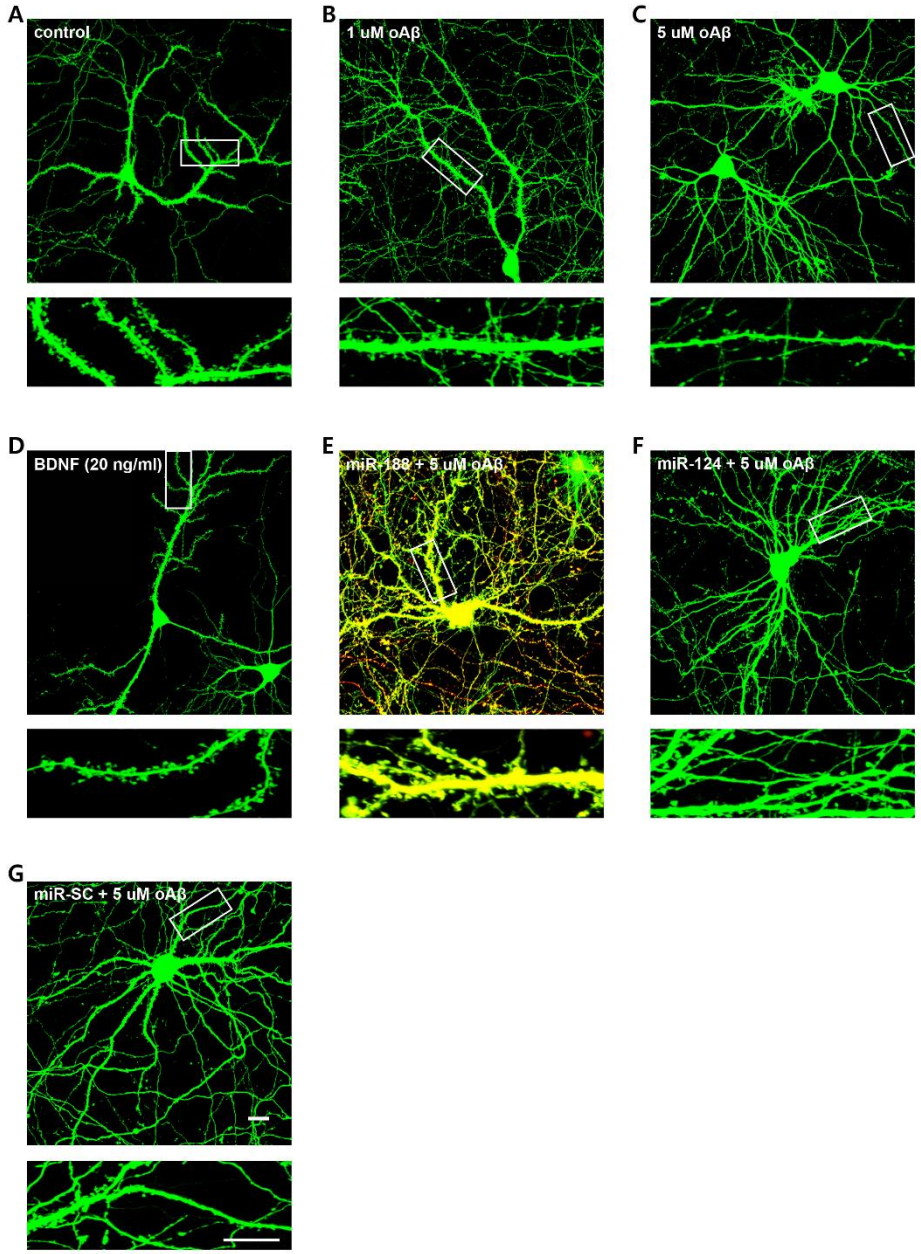
A
control
B
1 uM oAβ
C
5 uM oAβ
D
BDNF (20 ng/ml)
E
miR-188 + 5 uM oAβ
F
miR-124 + 5 uM oAβ
G
miR-SC + 5 uM oAβ

(H)

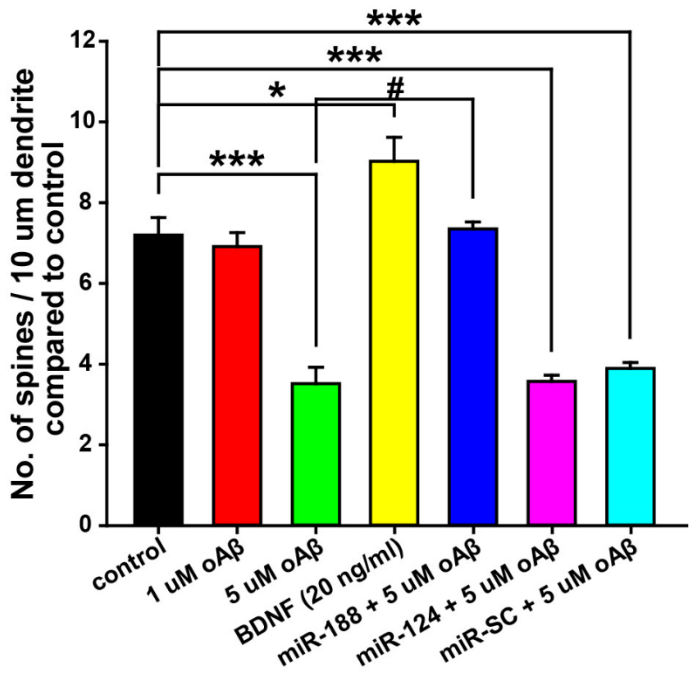

Figure 2-3. miR-188 rescued the reductions in dendritic spine densities induced by oAβ_{1-42} in rat primary hippocampal neuron cultures.

(A) - (G) Representative images of the dendritic spines of cultured primary hippocampal neurons at DIV 18-20 after treatment with oAβ_{1-42} alone or in combination with miR-188 (IRES-DsRed2), miR-124 or miR-SC oligonucleotides and IRES-mGFP vector at DIV 10-12. The dendritic segment outlined with the white box (upper) is magnified to delineate the spine morphology (bottom). Scale bars: 20 and 10 μm for the low- and high-magnification images, respectively. **(H)** Quantification of the spine density (the secondary dendritic spines within 50-100 μm of the soma were examined) of the cultured hippocampal neurons at DIV 18-20 after transfection at DIV

10-12. Treatment with 5 μM $oA\beta_{1-42}$ significantly reduced the numbers of dendritic spines per 10 μm of dendrites by 51.1% (3.5190 ± 0.4063, n=7, $^{***}p$=0.000906) compared to the mGFP-transfected controls (7.1957 ± 0.4355, n=10), and treatment with 1 μM $mA\beta_{1-42}$ did not alter dendritic spine density compared to that of the mGFP-transfected controls. Treatment with 5 μM $oA\beta_{1-42}$ and miR-188 reversed the reduction in the number of dendritic spines that was induced by 5 μM $oA\beta_{1-42}$ (7.3485 ± 0.17687, n=9, p=0.750663) compared to the mGFP-transfected controls. Treatment with 20 ng/ml BDNF significantly increased dendritic spine density (9.0241 ± 0.5922, n=9, $^{*}p$=0.011369), and treatment with 5 μM $oA\beta_{1-42}$ and miR-SC or miR-124 did not reverse the reduction in the number of dendritic spines that was induced by 5 μM $oA\beta_{1-42}$ (5 μM $oA\beta_{1-42}$ with miR-124, 3.5706 ± 0.1572, n=6, $^{***}p$=0.000007; 5 μM $oA\beta_{1-42}$ with miR-SC, 3.8923 ± 0.1458, n=8, $^{***}p$=0.000018) compared to the vehicle-treated controls. The statistical significance of the comparisons are indicated as follows: $^{***}p<0.001$ between the control and $oA\beta_{1-42}$ groups by independent t-tests or non-parametric Mann-Whitney U test; and $^{\#}p<0.001$ between the 5 μM $oA\beta_{1-42}$ and 5 μM $oA\beta_{1-42}$ with miR-188 groups (7.3485 ± 0.1768, n=9, $^{\#}p$=0.000175) by Mann-Whitney U test. The data are presented as the means ± the SEMs.

(A)

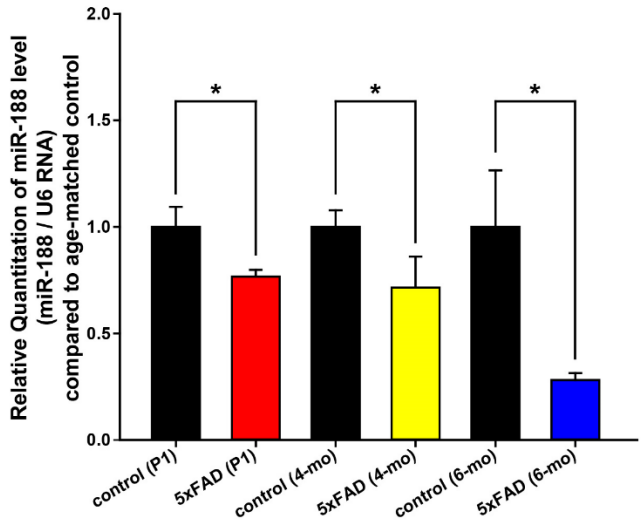

Figure 2-4. miR-188 was significantly downregulated in the hippocampi of the 5 x FAD mice compared to those of the wild-type mice.

(A) miR-188 expression in the hippocampal tissue of postnatal 1 (PND1) and 4- to 6-month-old 5 x FAD mice was examined by RT-qPCR. The expression of miR-188 was significantly downregulated in the hippocampi of the 5 x FAD mice (PND1: 0.7661 ± 0.0321, n=11 vs. age-matched controls, 1.0000 ± 0.0944, n=7, $^{*}p$=0.027259; 4 months of age: 0.7154 ± 0.1452, n=4 vs. age-matched control, 1.0000 ± 0.0777, n=5, $^{*}p$=0.037743; 6 months of age: 0.2811 ± 0.0327, n=3 vs. age-matched controls, 1.0000 ± 0.2654, n=4, $^{*}p$=0.013546). U6 snoRNA was used as a reference control. Statistical analyses were performed with independent t-tests or non-parametric Mann-Whitney U tests; $^{*}p<0.05$. The error bars indicate the SEM. PND1: wild-type n=7, 5 x FAD n=11. 4-mo: wild-type n=5, 5 x FAD n=4. 6-mo: wild-type n=4, 5 x FAD n=3.

(A)

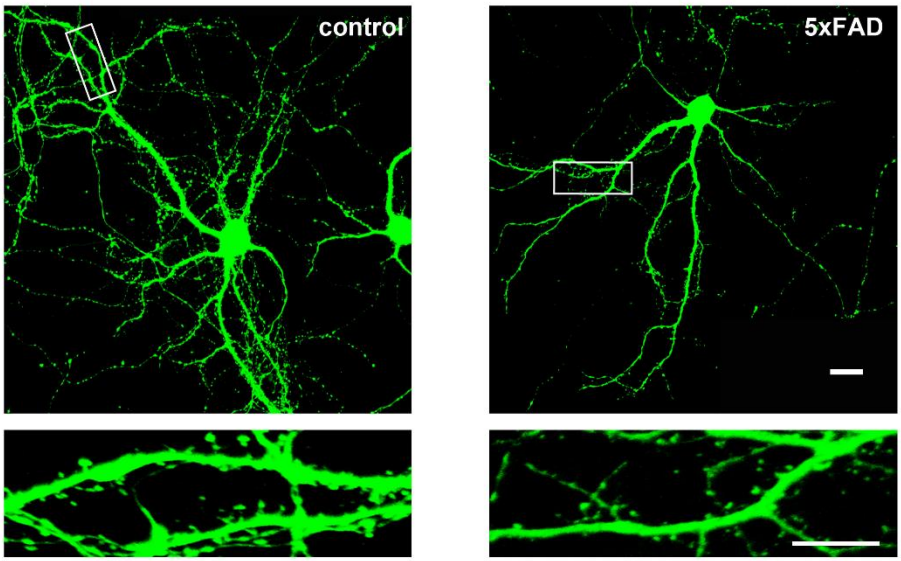
control
5xFAD

(B)

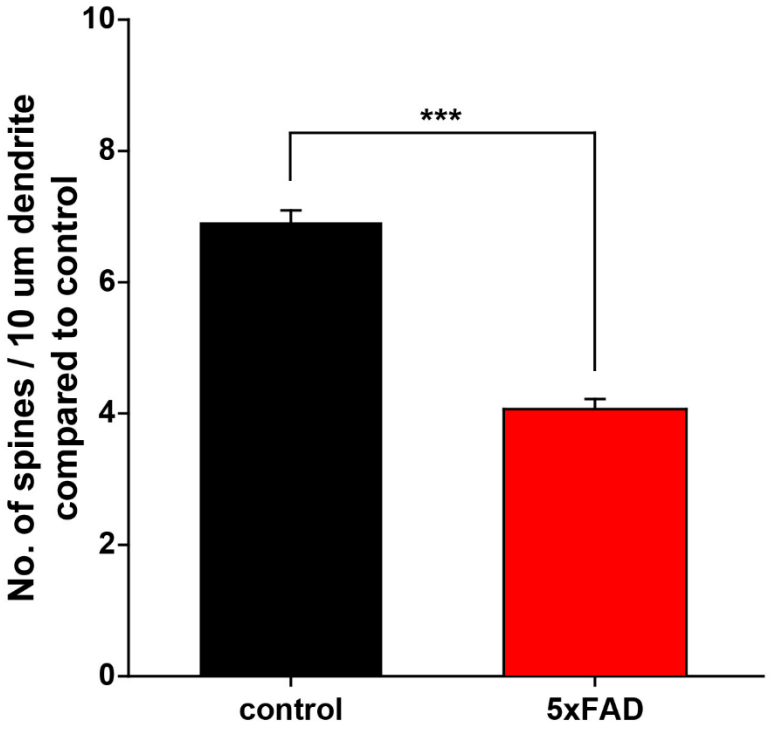
No. of spines / 10 um dendrite compared to control
10
8
6
4
2
0
***
control
5xFAD

Figure 2-5. Dendritic spine densities were reduced in the primary hippocampal neuron cultures of 5 x FAD mice.

(A) Representative images of dendritic spines in primary hippocampal neuron cultures of PND1 control and 5 x FAD mice at DIV 18-20 after transfection with IRES-mGFP vector at DIV 10-12. The dendritic segment outlined with a white box (upper) is magnified to delineate the spine morphology (bottom) with a 3x optic zoom. The scale bars indicate 20 and 10 μm in the low- and high-magnification images, respectively. **(B)** Quantification of the spine densities (secondary dendritic spines 50-100 μm from the soma) of PND1 cultured hippocampal neurons at DIV 18-20 after transfection at DIV 10-12 of the control and 5 x FAD mice. The neurons from the 5 x FAD mice exhibited a significant reduction in the number of dendritic spines per 10 μm of dendrites of 58.9% (4.0677 ± 0.1540, n=38) compared to the wild-type neurons of the control mice (6.9098 ± 0.1854, n=30; $^{***}p$=4.6444E-18). $^{***}p$<0.001 between the control and 5 x FAD groups by independent t-test. The data are presented as the means ± the SEM.

(A)

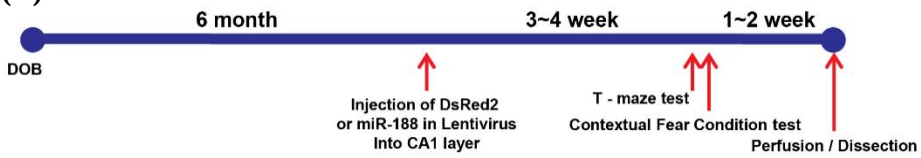

(B)

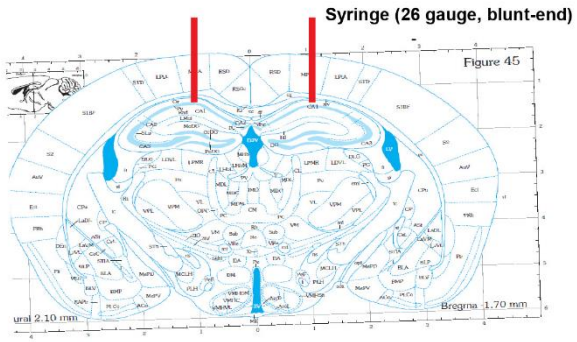

AP (Anterior/Posterior); - 0.17
ML (Medial/Lateral); ± 0.1
DV (Dorsal/Ventral); - 0.175

(C)

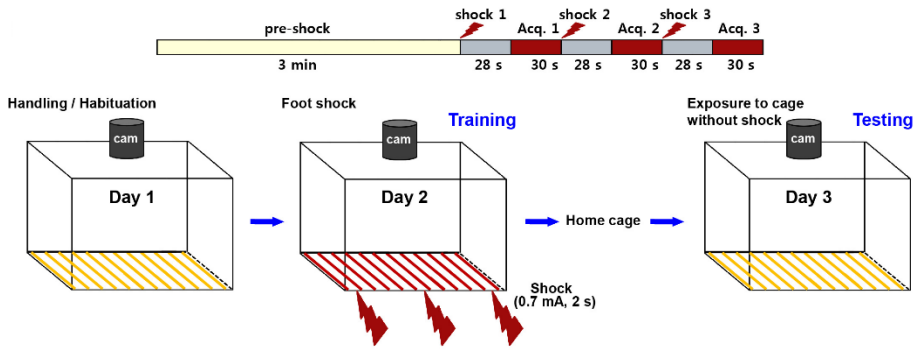

(D)

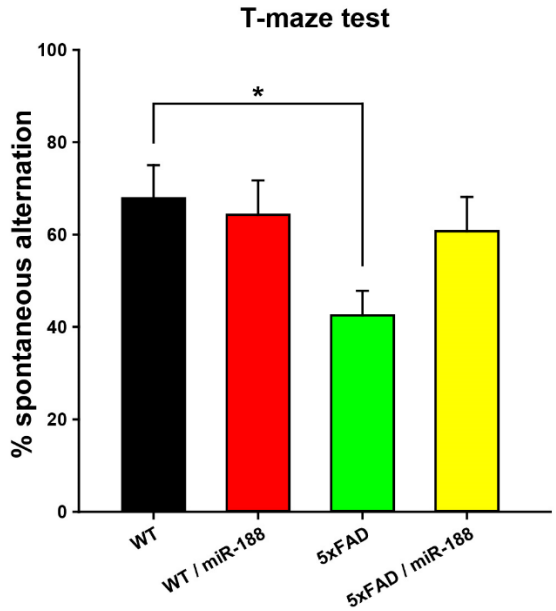
T-maze test
% spontaneous alternation
100
80
60
40
20
0
*
WT
WT / miR-188
5xFAD
5xFAD / miR-188

(E)

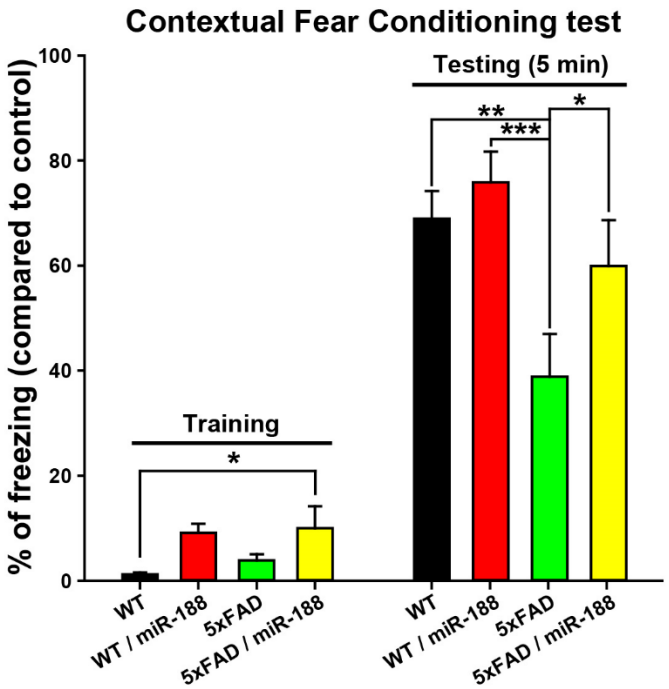
Contextual Fear Conditioning test
% of freezing (compared to control)
100
80
60
40
20
0
Training
*
Testing (5 min)
**
***
*
WT
WT / miR-188
5xFAD
5xFAD / miR-188
WT
WT / miR-188
5xFAD
5xFAD / miR-188

Figure 2-6. Viral-mediated expression of miR-188 in the hippocampus rescues the memory deficits of 5 x FAD mice.

(A) Experimental schedule of the overexpression of miR-188 in wild-type and 5 x FAD mice. **(B)** A coronal mouse brain atlas diagram of the localization of the miR-188 lentivirus injections in the mouse dorsal hippocampal CA1 region showing the stereotaxic grid, section number, structure labels and distance from bregma. **(C)** Illustration of the scheme for the contextual fear conditioning test. **(D)** The spatial working memory abilities of the mice were measured as their spontaneous alternation performances in the T-maze. Note that the 5 x FAD mice performed poorly (only slightly above the 40% chance level) compared to wild-type controls ($^{*}p<0.05$) and that the miR-188/5 x FAD mice performed at the level of the wild-types ($^{\#}p<0.05$ versus 5 x FAD). n = 7-10 mice per group. **(E)** The mice were trained with three foot shocks (0.7 mA at an interval of 2 sec) to induce contextual fear conditioning. The 5 x FAD mice exhibited significantly reduced levels of contextual freezing compared to the wild-type mice when tested 1 day after training. The freezing behavior of the miR-188/5 x FAD mice was completely rescued to the level of the wild-type mice ($^{*}p<0.05$, $^{**}p<0.01$ and $^{***}p<0.001$ versus 5 x FAD). n = 8-10 mice per group.

DISCUSSION

Numerous miRNAs have been reported to be downregulated in human AD brains (114, 128). However, few of the gene targets of these downregulated miRNA have been identified thus far. One target gene that has been identified APP, which is targeted by the miR-20a family and miR-101, and several of these miRNAs are downregulated in AD patients (51). Other miRNAs, including miR-9, regulate Aβ and BACE-1, and their expressions are also reduced in AD (53, 114). The loss of dendritic spines and synapses that occur in AD are well-known (128, 148). Spine growth is preceded by synapse formation, and newly formed spines increase in volume as they became stable (149).

The numbers of dendritic spines were reduced in the primary hippocampal neuron cultures that received o$A\beta_{1\text{-}42}$ treatment regardless of whether those cultures were created from the brains of wild-type or 5 x FAD mice. The 5 x FAD mouse is a well-known animal model of AD. The numbers of dendritic spines on the primary hippocampal neurons from SD rats and 5 x FAD mice were reduced compared to those of the wild-type mice by o$A\beta_{1\text{-}42}$ treatment (Figs. 2-3H and -5B).

The results of the present study may help to ameliorate the current lack of molecular targets and regulators that are suitable for reliably diagnosing AD in the early stages in which subtle alterations in synaptic efficacy and subtle synaptic dysfunctions occur.

Based on these results, I speculate that the dendritic spine alterations observed in AD are at least partial due to the deregulation of the expression of miR-188 and the subsequent uncontrolled Nrp-2 expression. Although additional work will be needed to elucidate the molecular mechanisms that are regulated by miR-188, I have provided evidence that the dysregulation of miRNAs may contribute to the synaptic dysfunctions that occur AD (Fig. 2-7).

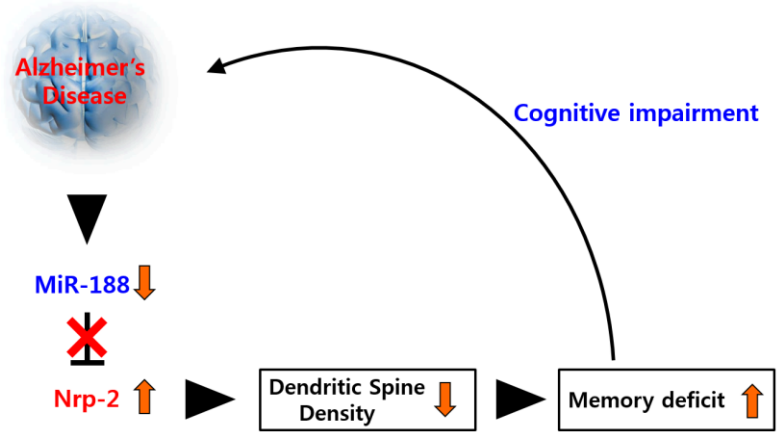

Figure 2-7. A hypothetical schematic diagram for regulatory mechanism of miR-188 in AD

Further research is particularly needed to elucidate the molecular mechanisms by which the expression of miR-188 is upregulated by synaptic activity and to elucidate the reason that miR-188 is downregulated in AD patients. The successful elucidation of these mechanisms will show that miR-188 is strong future candidate for use in diagnostic and therapeutic tools for the clinical treatment of AD.

REFERENCES

1. Carrington JC, Ambros V. Role of microRNAs in plant and animal development. Science. 2003;301(5631):336-8.
2. Bartel DP. MicroRNAs: genomics, biogenesis, mechanism, and function. Cell. 2004;116(2):281-97.
3. Lai EC. microRNAs: runts of the genome assert themselves. Current biology : CB. 2003;13(23):R925-36.
4. Murchison EP, Hannon GJ. miRNAs on the move: miRNA biogenesis and the RNAi machinery. Current opinion in cell biology. 2004;16(3):223-9.
5. Pfeffer S, Zavolan M, Grasser FA, Chien M, Russo JJ, Ju J, et al. Identification of virus-encoded microRNAs. Science. 2004;304(5671):734-6.
6. Shioya M, Obayashi S, Tabunoki H, Arima K, Saito Y, Ishida T, et al. Aberrant microRNA expression in the brains of neurodegenerative diseases: miR-29a decreased in Alzheimer disease brains targets neurone navigator 3. Neuropathology and applied neurobiology. 2010;36(4):320-30.
7. Ambros V. A hierarchy of regulatory genes controls a larva-to-adult developmental switch in C. elegans. Cell. 1989;57(1):49-57.
8. Ruvkun G, Giusto J. The Caenorhabditis elegans heterochronic gene lin-14 encodes a nuclear protein that forms a temporal developmental switch. Nature. 1989;338(6213):313-9.
9. Pasquinelli AE, Ruvkun G. Control of developmental timing by micrornas and their targets. Annual review of cell and developmental biology. 2002;18:495-513.
10. Cai Z, Liang TJ, Luo G. Effects of mutations of the initiation nucleotides on hepatitis C virus RNA replication in the cell. Journal of virology. 2004;78(7):3633-43.
11. Lee Y, Kim M, Han J, Yeom KH, Lee S, Baek SH, et al. MicroRNA genes are transcribed by RNA polymerase II. The EMBO journal. 2004;23(20):4051-60.
12. Borchert GM, Lanier W, Davidson BL. RNA polymerase III transcribes human microRNAs. Nature structural & molecular biology. 2006;13(12):1097-101.
13. Denli AM, Tops BB, Plasterk RH, Ketting RF, Hannon GJ. Processing of primary microRNAs by the Microprocessor complex. Nature. 2004;432(7014):231-5.
14. Gregory RI, Yan KP, Amuthan G, Chendrimada T, Doratotaj B, Cooch N, et al. The Microprocessor complex mediates the genesis of microRNAs. Nature. 2004;432(7014):235-40.
15. Han MH, Goud S, Song L, Fedoroff N. The Arabidopsis double-stranded RNA-

binding protein HYL1 plays a role in microRNA-mediated gene regulation. Proceedings of the National Academy of Sciences of the United States of America. 2004;101(4):1093-8.

16. Landthaler M, Yalcin A, Tuschl T. The human DiGeorge syndrome critical region gene 8 and Its D. melanogaster homolog are required for miRNA biogenesis. Current biology : CB. 2004;14(23):2162-7.
17. Lee Y, Ahn C, Han J, Choi H, Kim J, Yim J, et al. The nuclear RNase III Drosha initiates microRNA processing. Nature. 2003;425(6956):415-9.
18. Lee Y, Kim VN. Preparation and analysis of Drosha. Methods Mol Biol. 2005;309:17-28.
19. Yi R, Qin Y, Macara IG, Cullen BR. Exportin-5 mediates the nuclear export of pre-microRNAs and short hairpin RNAs. Genes & development. 2003;17(24):3011-6.
20. Bohnsack MT, Czaplinski K, Gorlich D. Exportin 5 is a RanGTP-dependent dsRNA-binding protein that mediates nuclear export of pre-miRNAs. RNA. 2004;10(2):185-91.
21. Kim VN. MicroRNA precursors in motion: exportin-5 mediates their nuclear export. Trends in cell biology. 2004;14(4):156-9.
22. Lund E, Guttinger S, Calado A, Dahlberg JE, Kutay U. Nuclear export of microRNA precursors. Science. 2004;303(5654):95-8.
23. Bernstein E, Caudy AA, Hammond SM, Hannon GJ. Role for a bidentate ribonuclease in the initiation step of RNA interference. Nature. 2001;409(6818):363-6.
24. Grishok A, Pasquinelli AE, Conte D, Li N, Parrish S, Ha I, et al. Genes and mechanisms related to RNA interference regulate expression of the small temporal RNAs that control C. elegans developmental timing. Cell. 2001;106(1):23-34.
25. Hutvagner G, McLachlan J, Pasquinelli AE, Balint E, Tuschl T, Zamore PD. A cellular function for the RNA-interference enzyme Dicer in the maturation of the let-7 small temporal RNA. Science. 2001;293(5531):834-8.
26. Ketting RF, Fischer SE, Bernstein E, Sijen T, Hannon GJ, Plasterk RH. Dicer functions in RNA interference and in synthesis of small RNA involved in developmental timing in C. elegans. Genes & development. 2001;15(20):2654-9.
27. Knight SW, Bass BL. A role for the RNase III enzyme DCR-1 in RNA interference and germ line development in Caenorhabditis elegans. Science. 2001;293(5538):2269-71.
28. Hammond SM, Bernstein E, Beach D, Hannon GJ. An RNA-directed nuclease

mediates post-transcriptional gene silencing in Drosophila cells. Nature. 2000;404(6775):293-6.
29. Martinez J, Patkaniowska A, Urlaub H, Luhrmann R, Tuschl T. Single-stranded antisense siRNAs guide target RNA cleavage in RNAi. Cell. 2002;110(5):563-74.
30. Schwarz DS, Zamore PD. Why do miRNAs live in the miRNP? Genes & development. 2002;16(9):1025-31.
31. Chi YH, Semmes OJ, Jeang KT. A proteomic study of TAR-RNA binding protein (TRBP)-associated factors. Cell & bioscience. 2011;1(1):9.
32. Chendrimada TP, Gregory RI, Kumaraswamy E, Norman J, Cooch N, Nishikura K, et al. TRBP recruits the Dicer complex to Ago2 for microRNA processing and gene silencing. Nature. 2005;436(7051):740-4.
33. Gregory RI, Chendrimada TP, Cooch N, Shiekhattar R. Human RISC couples microRNA biogenesis and posttranscriptional gene silencing. Cell. 2005;123(4):631-40.
34. Lim LP, Lau NC, Garrett-Engele P, Grimson A, Schelter JM, Castle J, et al. Microarray analysis shows that some microRNAs downregulate large numbers of target mRNAs. Nature. 2005;433(7027):769-73.
35. Cheng AM, Byrom MW, Shelton J, Ford LP. Antisense inhibition of human miRNAs and indications for an involvement of miRNA in cell growth and apoptosis. Nucleic acids research. 2005;33(4):1290-7.
36. Xu P, Guo M, Hay BA. MicroRNAs and the regulation of cell death. Trends in genetics : TIG. 2004;20(12):617-24.
37. Vo NK, Cambronne XA, Goodman RH. MicroRNA pathways in neural development and plasticity. Current opinion in neurobiology. 2010;20(4):457-65.
38. Yu JY, Chung KH, Deo M, Thompson RC, Turner DL. MicroRNA miR-124 regulates neurite outgrowth during neuronal differentiation. Experimental cell research. 2008;314(14):2618-33.
39. Park CS, Tang SJ. Regulation of microRNA expression by induction of bidirectional synaptic plasticity. Journal of molecular neuroscience : MN. 2009;38(1):50-6.
40. Rajasethupathy P, Fiumara F, Sheridan R, Betel D, Puthanveettil SV, Russo JJ, et al. Characterization of small RNAs in Aplysia reveals a role for miR-124 in constraining synaptic plasticity through CREB. Neuron. 2009;63(6):803-17.
41. Smalheiser NR, Lugli G. microRNA regulation of synaptic plasticity. Neuromolecular medicine. 2009;11(3):133-40.
42. Wayman GA, Davare M, Ando H, Fortin D, Varlamova O, Cheng HY, et al. An activity-regulated microRNA controls dendritic plasticity by down-regulating

p250GAP. Proceedings of the National Academy of Sciences of the United States of America. 2008;105(26):9093-8.

43. Yuste R, Bonhoeffer T. Morphological changes in dendritic spines associated with long-term synaptic plasticity. Annual review of neuroscience. 2001;24:1071-89.
44. Kim J, Inoue K, Ishii J, Vanti WB, Voronov SV, Murchison E, et al. A MicroRNA feedback circuit in midbrain dopamine neurons. Science. 2007;317(5842):1220-4.
45. Smirnova L, Grafe A, Seiler A, Schumacher S, Nitsch R, Wulczyn FG. Regulation of miRNA expression during neural cell specification. The European journal of neuroscience. 2005;21(6):1469-77.
46. Conaco C, Otto S, Han JJ, Mandel G. Reciprocal actions of REST and a microRNA promote neuronal identity. Proceedings of the National Academy of Sciences of the United States of America. 2006;103(7):2422-7.
47. Makeyev EV, Zhang J, Carrasco MA, Maniatis T. The MicroRNA miR-124 promotes neuronal differentiation by triggering brain-specific alternative pre-mRNA splicing. Molecular cell. 2007;27(3):435-48.
48. Schratt GM, Tuebing F, Nigh EA, Kane CG, Sabatini ME, Kiebler M, et al. A brain-specific microRNA regulates dendritic spine development. Nature. 2006;439(7074):283-9.
49. Siegel G, Obernosterer G, Fiore R, Oehmen M, Bicker S, Christensen M, et al. A functional screen implicates microRNA-138-dependent regulation of the depalmitoylation enzyme APT1 in dendritic spine morphogenesis. Nature cell biology. 2009;11(6):705-16.
50. Edbauer D, Neilson JR, Foster KA, Wang CF, Seeburg DP, Batterton MN, et al. Regulation of synaptic structure and function by FMRP-associated microRNAs miR-125b and miR-132. Neuron. 2010;65(3):373-84.
51. Hebert SS, Horre K, Nicolai L, Bergmans B, Papadopoulou AS, Delacourte A, et al. MicroRNA regulation of Alzheimer's Amyloid precursor protein expression. Neurobiology of disease. 2009;33(3):422-8.
52. Lukiw WJ. Micro-RNA speciation in fetal, adult and Alzheimer's disease hippocampus. Neuroreport. 2007;18(3):297-300.
53. Wang WX, Wilfred BR, Madathil SK, Tang G, Hu Y, Dimayuga J, et al. miR-107 regulates granulin/progranulin with implications for traumatic brain injury and neurodegenerative disease. The American journal of pathology. 2010;177(1):334-45.
54. Tansey EM. Not committing barbarisms: Sherrington and the synapse, 1897. Brain research bulletin. 1997;44(3):211-2.

55. Perkel DHaB, T. H. Neural coding. NRP Bulletin. 1968;6(3):221–348.
56. Mesulam MM. Neuroplasticity failure in Alzheimer's disease: bridging the gap between plaques and tangles. Neuron. 1999;24(3):521-9.
57. Nestler EJ, Barrot M, DiLeone RJ, Eisch AJ, Gold SJ, Monteggia LM. Neurobiology of depression. Neuron. 2002;34(1):13-25.
58. Woody CD, Black-Cleworth P. Differences in excitability of cortical neurons as a function of motor projection in conditioned cats. Journal of neurophysiology. 1973;36(6):1104-16.
59. Brons JF, Woody CD. Long-term changes in excitability of cortical neurons after Pavlovian conditioning and extinction. Journal of neurophysiology. 1980;44(3):605-15.
60. Bliss TV, Gardner-Medwin AR. Long-lasting potentiation of synaptic transmission in the dentate area of the unanaestetized rabbit following stimulation of the perforant path. The Journal of physiology. 1973;232(2):357-74.
61. Bliss TV, Lomo T. Long-lasting potentiation of synaptic transmission in the dentate area of the anaesthetized rabbit following stimulation of the perforant path. The Journal of physiology. 1973;232(2):331-56.
62. Bliss TV, Collingridge GL. A synaptic model of memory: long-term potentiation in the hippocampus. Nature. 1993;361(6407):31-9.
63. Hughes JR. Post-tetanic potentiation. Physiological reviews. 1958;38(1):91-113.
64. Citri A, Malenka RC. Synaptic plasticity: multiple forms, functions, and mechanisms. Neuropsychopharmacology : official publication of the American College of Neuropsychopharmacology. 2008;33(1):18-41.
65. Rumpel S, LeDoux J, Zador A, Malinow R. Postsynaptic receptor trafficking underlying a form of associative learning. Science. 2005;308(5718):83-8.
66. Gruart A, Munoz MD, Delgado-Garcia JM. Involvement of the CA3-CA1 synapse in the acquisition of associative learning in behaving mice. The Journal of neuroscience : the official journal of the Society for Neuroscience. 2006;26(4):1077-87.
67. Whitlock JR, Heynen AJ, Shuler MG, Bear MF. Learning induces long-term potentiation in the hippocampus. Science. 2006;313(5790):1093-7.
68. Chen H, Bagri A, Zupicich JA, Zou Y, Stoeckli E, Pleasure SJ, et al. Neuropilin-2 regulates the development of selective cranial and sensory nerves and hippocampal mossy fiber projections. Neuron. 2000;25(1):43-56.
69. Kolodkin AL, Levengood DV, Rowe EG, Tai YT, Giger RJ, Ginty DD. Neuropilin is a semaphorin III receptor. Cell. 1997;90(4):753-62.
70. Chen H, Chedotal A, He Z, Goodman CS, Tessier-Lavigne M. Neuropilin-2, a

novel member of the neuropilin family, is a high affinity receptor for the semaphorins Sema E and Sema IV but not Sema III. Neuron. 1997;19(3):547-59.
71. He Z, Tessier-Lavigne M. Neuropilin is a receptor for the axonal chemorepellent Semaphorin III. Cell. 1997;90(4):739-51.
72. Neufeld G, Cohen T, Shraga N, Lange T, Kessler O, Herzog Y. The neuropilins: multifunctional semaphorin and VEGF receptors that modulate axon guidance and angiogenesis. Trends in cardiovascular medicine. 2002;12(1):13-9.
73. Tran TS, Rubio ME, Clem RL, Johnson D, Case L, Tessier-Lavigne M, et al. Secreted semaphorins control spine distribution and morphogenesis in the postnatal CNS. Nature. 2009;462(7276):1065-9.
74. Chen C, Li M, Chai H, Yang H, Fisher WE, Yao Q. Roles of neuropilins in neuronal development, angiogenesis, and cancers. World journal of surgery. 2005;29(3):271-5.
75. Gu C, Limberg BJ, Whitaker GB, Perman B, Leahy DJ, Rosenbaum JS, et al. Characterization of neuropilin-1 structural features that confer binding to semaphorin 3A and vascular endothelial growth factor 165. J Biol Chem. 2002;277(20):18069-76.
76. Sahay A, Kim CH, Sepkuty JP, Cho E, Huganir RL, Ginty DD, et al. Secreted semaphorins modulate synaptic transmission in the adult hippocampus. The Journal of neuroscience : the official journal of the Society for Neuroscience. 2005;25(14):3613-20.
77. Cummings JL. Cognitive and behavioral heterogeneity in Alzheimer's disease: seeking the neurobiological basis. Neurobiology of aging. 2000;21(6):845-61.
78. Scheff SW, Price DA. Synaptic pathology in Alzheimer's disease: a review of ultrastructural studies. Neurobiology of aging. 2003;24(8):1029-46.
79. Selkoe DJ. Alzheimer's disease is a synaptic failure. Science. 2002;298(5594):789-91.
80. Arendt T. Disturbance of neuronal plasticity is a critical pathogenetic event in Alzheimer's disease. International journal of developmental neuroscience : the official journal of the International Society for Developmental Neuroscience. 2001;19(3):231-45.
81. Arendt T, Bruckner MK, Gertz HJ, Marcova L. Cortical distribution of neurofibrillary tangles in Alzheimer's disease matches the pattern of neurons that retain their capacity of plastic remodelling in the adult brain. Neuroscience. 1998;83(4):991-1002.
82. Lin LH, Bock S, Carpenter K, Rose M, Norden JJ. Synthesis and transport of GAP-43 in entorhinal cortex neurons and perforant pathway during lesion-

induced sprouting and reactive synaptogenesis. Brain research Molecular brain research. 1992;14(1-2):147-53.

83. Okuno H, Tokuyama W, Li YX, Hashimoto T, Miyashita Y. Quantitative evaluation of neurotrophin and trk mRNA expression in visual and limbic areas along the occipito-temporo-hippocampal pathway in adult macaque monkeys. The Journal of comparative neurology. 1999;408(3):378-98.
84. Hardy J, Selkoe DJ. The amyloid hypothesis of Alzheimer's disease: progress and problems on the road to therapeutics. Science. 2002;297(5580):353-6.
85. Glenner GG, Wong CW. Alzheimer's disease and Down's syndrome: sharing of a unique cerebrovascular amyloid fibril protein. Biochemical and biophysical research communications. 1984;122(3):1131-5.
86. Kang J, Lemaire HG, Unterbeck A, Salbaum JM, Masters CL, Grzeschik KH, et al. The precursor of Alzheimer's disease amyloid A4 protein resembles a cell-surface receptor. Nature. 1987;325(6106):733-6.
87. Esch FS, Keim PS, Beattie EC, Blacher RW, Culwell AR, Oltersdorf T, et al. Cleavage of amyloid beta peptide during constitutive processing of its precursor. Science. 1990;248(4959):1122-4.
88. Seubert P, Oltersdorf T, Lee MG, Barbour R, Blomquist C, Davis DL, et al. Secretion of beta-amyloid precursor protein cleaved at the amino terminus of the beta-amyloid peptide. Nature. 1993;361(6409):260-3.
89. Pike CJ, Walencewicz-Wasserman AJ, Kosmoski J, Cribbs DH, Glabe CG, Cotman CW. Structure-activity analyses of beta-amyloid peptides: contributions of the beta 25-35 region to aggregation and neurotoxicity. Journal of neurochemistry. 1995;64(1):253-65.
90. Llibre Rodriguez JJ, Ferri CP, Acosta D, Guerra M, Huang Y, Jacob KS, et al. Prevalence of dementia in Latin America, India, and China: a population-based cross-sectional survey. Lancet. 2008;372(9637):464-74.
91. Brookmeyer R, Johnson E, Ziegler-Graham K, Arrighi HM. Forecasting the global burden of Alzheimer's disease. Alzheimer's & dementia : the journal of the Alzheimer's Association. 2007;3(3):186-91.
92. Lambert TJ, Storm DR, Sullivan JM. MicroRNA132 modulates short-term synaptic plasticity but not basal release probability in hippocampal neurons. PloS one. 2010;5(12):e15182.
93. Kotaleski JH, Blackwell KT. Modelling the molecular mechanisms of synaptic plasticity using systems biology approaches. Nature reviews Neuroscience. 2010;11(4):239-51.
94. Kosik KS. The neuronal microRNA system. Nature reviews Neuroscience.

2006;7(12):911-20.
95. Guo H, Ingolia NT, Weissman JS, Bartel DP. Mammalian microRNAs predominantly act to decrease target mRNA levels. Nature. 2010;466(7308):835-40.
96. Cohen JE, Lee PR, Chen S, Li W, Fields RD. MicroRNA regulation of homeostatic synaptic plasticity. Proceedings of the National Academy of Sciences of the United States of America. 2011;108(28):11650-5.
97. Liu SJ, Lachamp P. The activation of excitatory glutamate receptors evokes a long-lasting increase in the release of GABA from cerebellar stellate cells. The Journal of neuroscience : the official journal of the Society for Neuroscience. 2006;26(36):9332-9.
98. Fonseca R, Vabulas RM, Hartl FU, Bonhoeffer T, Nagerl UV. A balance of protein synthesis and proteasome-dependent degradation determines the maintenance of LTP. Neuron. 2006;52(2):239-45.
99. Karpova A, Mikhaylova M, Thomas U, Knopfel T, Behnisch T. Involvement of protein synthesis and degradation in long-term potentiation of Schaffer collateral CA1 synapses. The Journal of neuroscience : the official journal of the Society for Neuroscience. 2006;26(18):4949-55.
100. Fonseca R, Nagerl UV, Bonhoeffer T. Neuronal activity determines the protein synthesis dependence of long-term potentiation. Nature neuroscience. 2006;9(4):478-80.
101. Yokose J, Ishizuka T, Yoshida T, Aoki J, Koyanagi Y, Yawo H. Lineage analysis of newly generated neurons in organotypic culture of rat hippocampus. Neuroscience research. 2011;69(3):223-33.
102. Spruston N. Pyramidal neurons: dendritic structure and synaptic integration. Nature reviews Neuroscience. 2008;9(3):206-21.
103. Rubinson DA, Dillon CP, Kwiatkowski AV, Sievers C, Yang L, Kopinja J, et al. A lentivirus-based system to functionally silence genes in primary mammalian cells, stem cells and transgenic mice by RNA interference. Nature genetics. 2003;33(3):401-6.
104. Martinat C, Bacci JJ, Leete T, Kim J, Vanti WB, Newman AH, et al. Cooperative transcription activation by Nurr1 and Pitx3 induces embryonic stem cell maturation to the midbrain dopamine neuron phenotype. Proceedings of the National Academy of Sciences of the United States of America. 2006;103(8):2874-9.
105. Lau P, Hudson LD. MicroRNAs in neural cell differentiation. Brain Res. 2010;1338:14-9.

106. Benoit ME, Tenner AJ. Complement protein C1q-mediated neuroprotection is correlated with regulation of neuronal gene and microRNA expression. The Journal of neuroscience : the official journal of the Society for Neuroscience. 2011;31(9):3459-69.
107. Baek D, Villen J, Shin C, Camargo FD, Gygi SP, Bartel DP. The impact of microRNAs on protein output. Nature. 2008;455(7209):64-71.
108. Shimakawa S, Suzuki S, Miyamoto R, Takitani K, Tanaka K, Tanabe T, et al. Neuropilin-2 is overexpressed in the rat brain after limbic seizures. Brain research. 2002;956(1):67-73.
109. Naska S, Lin DC, Miller FD, Kaplan DR. p75NTR is an obligate signaling receptor required for cues that cause sympathetic neuron growth cone collapse. Molecular and cellular neurosciences. 2010;45(2):108-20.
110. Gluzman-Poltorak Z, Cohen T, Shibuya M, Neufeld G. Vascular endothelial growth factor receptor-1 and neuropilin-2 form complexes. The Journal of biological chemistry. 2001;276(22):18688-94.
111. Lee JS, Jang DJ, Lee N, Ko HG, Kim H, Kim YS, et al. Induction of neuronal vascular endothelial growth factor expression by cAMP in the dentate gyrus of the hippocampus is required for antidepressant-like behaviors. The Journal of neuroscience : the official journal of the Society for Neuroscience. 2009;29(26):8493-505.
112. Demyanenko GP, Riday TT, Tran TS, Dalal J, Darnell EP, Brennaman LH, et al. NrCAM deletion causes topographic mistargeting of thalamocortical axons to the visual cortex and disrupts visual acuity. The Journal of neuroscience : the official journal of the Society for Neuroscience. 2011;31(4):1545-58.
113. Schonrock N, Matamales M, Ittner LM, Gotz J. MicroRNA networks surrounding APP and amyloid-beta metabolism - Implications for Alzheimer's disease. Experimental neurology. 2011.
114. Hebert SS, Horre K, Nicolai L, Papadopoulou AS, Mandemakers W, Silahtaroglu AN, et al. Loss of microRNA cluster miR-29a/b-1 in sporadic Alzheimer's disease correlates with increased BACE1/beta-secretase expression. Proceedings of the National Academy of Sciences of the United States of America. 2008;105(17):6415-20.
115. Boissonneault V, Plante I, Rivest S, Provost P. MicroRNA-298 and microRNA-328 regulate expression of mouse beta-amyloid precursor protein-converting enzyme 1. The Journal of biological chemistry. 2009;284(4):1971-81.
116. Long JM, Lahiri DK. MicroRNA-101 downregulates Alzheimer's amyloid-beta precursor protein levels in human cell cultures and is differentially expressed.

Biochemical and biophysical research communications. 2011;404(4):889-95.
117. Carrettiero DC, Hernandez I, Neveu P, Papagiannakopoulos T, Kosik KS. The cochaperone BAG2 sweeps paired helical filament- insoluble tau from the microtubule. The Journal of neuroscience : the official journal of the Society for Neuroscience. 2009;29(7):2151-61.
118. Hebert SS, Papadopoulou AS, Smith P, Galas MC, Planel E, Silahtaroglu AN, et al. Genetic ablation of Dicer in adult forebrain neurons results in abnormal tau hyperphosphorylation and neurodegeneration. Human molecular genetics. 2010;19(20):3959-69.
119. Ponomarev ED, Veremeyko T, Barteneva N, Krichevsky AM, Weiner HL. MicroRNA-124 promotes microglia quiescence and suppresses EAE by deactivating macrophages via the C/EBP-alpha-PU.1 pathway. Nature medicine. 2011;17(1):64-70.
120. Taganov KD, Boldin MP, Chang KJ, Baltimore D. NF-kappaB-dependent induction of microRNA miR-146, an inhibitor targeted to signaling proteins of innate immune responses. Proceedings of the National Academy of Sciences of the United States of America. 2006;103(33):12481-6.
121. Perry MM, Williams AE, Tsitsiou E, Larner-Svensson HM, Lindsay MA. Divergent intracellular pathways regulate interleukin-1beta-induced miR-146a and miR-146b expression and chemokine release in human alveolar epithelial cells. FEBS letters. 2009;583(20):3349-55.
122. Vilardo E, Barbato C, Ciotti M, Cogoni C, Ruberti F. MicroRNA-101 regulates amyloid precursor protein expression in hippocampal neurons. The Journal of biological chemistry. 2010;285(24):18344-51.
123. Lukiw WJ, Zhao Y, Cui JG. An NF-kappaB-sensitive micro RNA-146a-mediated inflammatory circuit in Alzheimer disease and in stressed human brain cells. The Journal of biological chemistry. 2008;283(46):31315-22.
124. Fang M, Wang J, Zhang X, Geng Y, Hu Z, Rudd JA, et al. The miR-124 regulates the expression of BACE1/beta-secretase correlated with cell death in Alzheimer's disease. Toxicology letters. 2012;209(1):94-105.
125. Cimmino A, Calin GA, Fabbri M, Iorio MV, Ferracin M, Shimizu M, et al. miR-15 and miR-16 induce apoptosis by targeting BCL2. Proceedings of the National Academy of Sciences of the United States of America. 2005;102(39):13944-9.
126. Schipper HM, Maes OC, Chertkow HM, Wang E. MicroRNA expression in Alzheimer blood mononuclear cells. Gene regulation and systems biology. 2007;1:263-74.
127. Villa C, Fenoglio C, De Riz M, Clerici F, Marcone A, Benussi L, et al. Role of

hnRNP-A1 and miR-590-3p in neuronal death: genetics and expression analysis in patients with Alzheimer disease and frontotemporal lobar degeneration. Rejuvenation research. 2011;14(3):275-81.

128. Cogswell JP, Ward J, Taylor IA, Waters M, Shi Y, Cannon B, et al. Identification of miRNA changes in Alzheimer's disease brain and CSF yields putative biomarkers and insights into disease pathways. J Alzheimers Dis. 2008;14(1):27-41.
129. Lee K, Kim JH, Kwon OB, An K, Ryu J, Cho K, et al. An activity-regulated microRNA, miR-188, controls dendritic plasticity and synaptic transmission by downregulating neuropilin-2. The Journal of neuroscience : the official journal of the Society for Neuroscience. 2012;32(16):5678-87.
130. Oakley H, Cole SL, Logan S, Maus E, Shao P, Craft J, et al. Intraneuronal beta-amyloid aggregates, neurodegeneration, and neuron loss in transgenic mice with five familial Alzheimer's disease mutations: potential factors in amyloid plaque formation. The Journal of neuroscience : the official journal of the Society for Neuroscience. 2006;26(40):10129-40.
131. Kim J, Lee S, Park K, Hong I, Song B, Son G, et al. Amygdala depotentiation and fear extinction. Proceedings of the National Academy of Sciences of the United States of America. 2007;104(52):20955-60.
132. Granic I, Masman MF, Kees Mulder C, Nijholt IM, Naude PJ, de Haan A, et al. LPYFDa neutralizes amyloid-beta-induced memory impairment and toxicity. Journal of Alzheimer's disease : JAD. 2010;19(3):991-1005.
133. Moon M, Choi JG, Nam DW, Hong HS, Choi YJ, Oh MS, et al. Ghrelin ameliorates cognitive dysfunction and neurodegeneration in intrahippocampal amyloid-beta1-42 oligomer-injected mice. Journal of Alzheimer's disease : JAD. 2011;23(1):147-59.
134. Deacon RM, Rawlins JN. T-maze alternation in the rodent. Nature protocols. 2006;1(1):7-12.
135. Kimura R, Ohno M. Impairments in remote memory stabilization precede hippocampal synaptic and cognitive failures in 5XFAD Alzheimer mouse model. Neurobiology of disease. 2009;33(2):229-35.
136. Kimura R, Devi L, Ohno M. Partial reduction of BACE1 improves synaptic plasticity, recent and remote memories in Alzheimer's disease transgenic mice. Journal of neurochemistry. 2010;113(1):248-61.
137. Selkoe DJ. Alzheimer's disease: genes, proteins, and therapy. Physiological reviews. 2001;81(2):741-66.
138. Lindholm D, Wootz H, Korhonen L. ER stress and neurodegenerative diseases.

Cell death and differentiation. 2006;13(3):385-92.
139. Fumagalli F, Racagni G, Riva MA. The expanding role of BDNF: a therapeutic target for Alzheimer's disease? The pharmacogenomics journal. 2006;6(1):8-15.
140. Li M, Dai FR, Du XP, Yang QD, Zhang X, Chen Y. Infusion of BDNF into the nucleus accumbens of aged rats improves cognition and structural synaptic plasticity through PI3K-ILK-Akt signaling. Behavioural brain research. 2012;231(1):146-53.
141. Arancibia S, Silhol M, Mouliere F, Meffre J, Hollinger I, Maurice T, et al. Protective effect of BDNF against beta-amyloid induced neurotoxicity in vitro and in vivo in rats. Neurobiology of disease. 2008;31(3):316-26.
142. Walsh DM, Klyubin I, Fadeeva JV, Cullen WK, Anwyl R, Wolfe MS, et al. Naturally secreted oligomers of amyloid beta protein potently inhibit hippocampal long-term potentiation in vivo. Nature. 2002;416(6880):535-9.
143. Cleary JP, Walsh DM, Hofmeister JJ, Shankar GM, Kuskowski MA, Selkoe DJ, et al. Natural oligomers of the amyloid-beta protein specifically disrupt cognitive function. Nature neuroscience. 2005;8(1):79-84.
144. Lesne S, Koh MT, Kotilinek L, Kayed R, Glabe CG, Yang A, et al. A specific amyloid-beta protein assembly in the brain impairs memory. Nature. 2006;440(7082):352-7.
145. Hsieh H, Boehm J, Sato C, Iwatsubo T, Tomita T, Sisodia S, et al. AMPAR removal underlies Abeta-induced synaptic depression and dendritic spine loss. Neuron. 2006;52(5):831-43.
146. Shankar GM, Bloodgood BL, Townsend M, Walsh DM, Selkoe DJ, Sabatini BL. Natural oligomers of the Alzheimer amyloid-beta protein induce reversible synapse loss by modulating an NMDA-type glutamate receptor-dependent signaling pathway. The Journal of neuroscience : the official journal of the Society for Neuroscience. 2007;27(11):2866-75.
147. Fanselow MS. Contextual fear, gestalt memories, and the hippocampus. Behavioural brain research. 2000;110(1-2):73-81.
148. Knobloch M, Mansuy IM. Dendritic spine loss and synaptic alterations in Alzheimer's disease. Molecular neurobiology. 2008;37(1):73-82.
149. Knott GW, Holtmaat A, Wilbrecht L, Welker E, Svoboda K. Spine growth precedes synapse formation in the adult neocortex in vivo. Nature neuroscience. 2006;9(9):1117-24.

국문 초록

서론: 다양한 생물계통에서, 마이크로알엔에이는 세포 내 유전자의 전사를 조절함으로써 전사 후 조절인자로서 기능을 한다고 알려져 있다. 특히, 마이크로알엔에이는 중추신경계에서 발달, 생존, 기능에 관여하며 가소성을 조절하고 있다. 마이크로알엔에이의 조절기능에 대한 상당한 증거들에도 불구하고, 시냅스 전도나 시냅스 가소성의 조절 및 기능에 관여하는 마이크로알엔에이 종류들은 아직 많이 알려져 있지 않다. 알츠하이머병과 같은 신경퇴행성 질환은 시냅스 기능의 저하와 신경세포 소실로 인해 발병되는 질병이다. 하지만, 마이크로알엔에이가 알츠하이머병에서 시냅스 가소성을 조절하는 조절자로써 기능하는지에 대해서는 아직도 잘 알려져 있지 않다.

방법: 랫트의 해마 조직에 장기강화 유도 후, 마이크로알엔에이 마이크로어레이 및 RT-qPCR을 수행하여 마이크로알엔에이들의 발현 변화를 확인하였다. 그 후, 생물정보학적 프로그램을 사용하여 증가/감소를 보이는 마이크로알엔에이들의 타겟 유전자를 예상하였다. miR-188과 뉴로필린-2의 직접적 결합을 확인하기 위해, 루시퍼레이즈 효소활성을 측정하였다. miR-188이 뉴로필린-2의 발현을 조절함으로써 시냅스 가소성에 영향을 주는지를 확인하기 위해, 수상돌기 가시 수를 측정하였다.

다음으로, 알츠하이머병 환자와 정상 대조군 뇌 및 알츠하이머 동물모델 뇌의 miR-188의 발현 변화를 RT-qPCR을 통하여

확인하였으며, 조직면역염색법을 이용하여 타겟 유전자인 뉴로필린-2의 단백질 발현을 확인하였다. 그리고, 올리고체 $A\beta_{1-42}$ 처리에 의해 miR-188의 발현 변화가 있는지를 확인하기 위하여 RT-qPCR을 수행하였다. 또한, 올리고체 $A\beta_{1-42}$ 처리에 의한 수상돌기 가시 수에 미치는 영향을 조사하였다. 마지막으로, 생체 내에서 miR-188의 인지 기능에 있어서의 역할을 확인하기 위해, 알츠하이머병 동물 모델인 5 x FAD 마우스에서 miR-188을 과발현하는 바이러스를 주입한 3주 후, 해마의존적 행동실험을 통하여 손상된 기억을 회복하는지를 측정하였다.

결과: 본 연구에서, miR-188의 발현이 장기 강화의 유도에 의해 상향조절되는 것으로 밝혀졌다. miR-188의 타겟 물질 중 하나인 뉴로필린-2의 단백질 발현은 장기강화 유도 시 감소되었다. miR-188를 처치하였을 때, 뉴로필린-2의 wild-type 3' UTR에 대한 루시퍼레이즈 효소활성이 감소되었지만, 뉴로필린-2의 mutant 3' UTR에서는 miR-188의 처치에 의한 효소활성의 변화가 없었다. Nrp-2는 Sema3F와 VEGF에 대한 수용체로서 작용하며, 수상돌기 가시의 발달과 시냅스 구조의 음성적 조절자로 잘 알려져 있다. 게다가, miR-188은 랫트 1차 해마 신경세포 배양에서 뉴로필린-2의 발현에 의해 유도된 수상돌기 가시의 감소를 정상수준으로 회복시켰다.

다음으로, miR-188이 알츠하이머병의 병인에 관여하는지를 조사하였다. 알츠하이머병 환자로부터 얻어진 대뇌피질과 해마 부위에서 정상대조군에 비해 miR-188의 발현이 유의하게 감소되어 있었다. 또한,

올리고체 $A\beta_{1-42}$의 처치가 miR-188의 발현을 현저히 감소시켰으며, 이에 반해 신경영양성 인자인 BDNF의 처치에서는 1차 해마 신경세포 배양에서 miR-188의 발현을 증가시켰다. 1차 해마 신경세포 배양에서, 올리고체 $A\beta_{1-42}$의 처리에 의해 감소된 수상돌기 가시 수가 miR-188의 보충으로 회복되었다. 게다가, 해마의 CA1 부위로 miR-188을 주입해 주었을 때, 5 x FAD 마우스에서 인지기능이 유의적으로 회복되었다.

결론: 시냅스 활성에 의하여 발현이 조절되는 마이크로알엔에이인 miR-188이 뉴로필린-2의 발현을 조절함으로써 수상돌기 가시의 수를 조절한다는 것을 보여준다. 뉴로필린-2는 수상돌기 가시의 형성과 시냅스 전달의 음성적 조절자로 알려져 있다. 또한, 알츠하이머병 환자 및 동물 모델의 뇌에서 관찰되는 miR-188의 감소가 알츠하이머병의 인지 기능 저하에 관여하리라고 사료된다.

위 결과를 통합하여 볼 때에, miR-188이 알츠하이머병의 치료에 대한 타겟이 될 수 있으며, 또한 질병 진단 바이오 마커로서 개발될 가능성을 가지는 것으로 생각된다.

주요어: 마이크로알엔에이, 시냅스 가소성, 뉴로필린 2, 인지기능 손상, 알츠하이머병

학 번: 2008-31030